LIMIT CYCLES IN TWO DIMENSIONAL SYSTEMS OF ORDINARY DIFFERENTIAL EQUATIONS

by

Ashley Rowe

A thesis submitted to the faculty of
The University of North Carolina at Charlotte
in partial fulfillment of the requirements
for the degree of Master of Science in
Mathematics

Charlotte

2018

Approved by:

_____

Dr. Douglas Shafer

_____

Dr. Kevin McGoff

_____

Dr. Boris Vainberg

ABSTRACT

ASHLEY ROWE. Limit Cycles in Two Dimensional Systems of Ordinary Differential Equations. (Under the direction of DR. DOUGLAS SHAFER)

This thesis concerns cycles, i.e., topological ovals, in the phase portraits of systems of first order ordinary differential equations in the plane, with an emphasis on limit cycles, cycles that are isolated from all other cycles. These are of fundamental importance because when asymptotically stable they correspond to limiting periodic behavior in the underlying system of differential equations. We treat basic theorems, with their proofs, concerning existence, non-existence, and unicity of cycles, and culminate with a general theorem guaranteeing existence of an asymptotically stable limit cycle in the phase portrait of systems of first order equations that correspond to differential equations of the form $\ddot{x} + f(x)\dot{x} + g(x) = 0$. The thesis includes examples that illustrate the theorems, including the historically important Volterra-Lotka family and the van der Pol oscillator.

ACKNOWLEDGMENTS

I would like to thank my thesis advisor Dr. Shafer of the Department of Mathematics and Statistics at the University of North Carolina at Charlotte. The time and energy Dr. Shafer put into helping me with this thesis was beyond compare. His office was always open whenever I ran into trouble or had a question. Without his many hours of proof reading, editing, and advise, this thesis would not have been possible.

Distinguished members of this committee headed by Dr. Douglas Shafer together with Dr. Kevin McGoff and Dr. Boris Vainberg for the approval of my work and recommendations.

I would also like to express my gratitude to my family and fiancé for providing me with unfailing support and continuous encouragement throughout my years of study and through the process of researching and writing this thesis. This accomplishment would not have been possible without them.

Most importantly, I would like to thank God for giving me the wisdom, perseverance, and good health in order to finish this thesis and program.

TABLE OF CONTENTS

LIST OF FIGURES

CHAPTER 1: INTRODUCTION

1.1 A General Summary

This thesis is dedicated to the study of limit cycles in two-dimensional systems of ordinary differential equations and is expository in nature. The study of limit cycles was first researched by French mathematician and physicist, Henri Poincaré. In this thesis, we will look at limit cycles as isolated, closed trajectories in the phase space. These trajectories have at least one other trajectory that spirals onto it as time approaches either infinity or negative infinity. Limit cycles are important because they model self-sustained oscillations such as heart beats, vibrations in bridges, and many other real world situations. In this paper we will study how a limit cycle is formed, theorems regarding existence and non-existence, and some real world problems where we can see these cycles. While this thesis will only cover a small portion of the theory of limit cycles, there are whole books devoted solely to limit cycles (e.g., [16]). Some areas that we will not cover in this theorem, but are still important in the study of limit cycles include the creation and annihilation of cycles in parametrized families of systems of ordinary differential equations.

1.2 Existence and Uniqueness

There are many different existence and uniqueness theorems concerning solutions of initial value problems associated with first order ordinary differential equations.

These theorems all have varying hypothesis and conclusions. While the existence and uniqueness theorem that will be used below is far from the most general of these, it is adequate for our purposes in this thesis.

Theorem 1. Suppose $E \in \mathbb{R}^n$ is an open set and $f : E \to \mathbb{R}^n$ is a C^r mapping, $r \geq 1$ Then for any $x_0 \in E$, the initial value problem (IVP)

$$\begin{aligned} \dot{x} &= f(x) \\ x(0) &= x_0 \end{aligned} \tag{1}$$

has a solution on some open interval I containing 0, and any two such solutions agree on their common domain.

For the purpose of this thesis, let $\Phi(t, x_0)$ denote the unique solution of (1) on its maximum interval of existence I about $t = 0$. In fact, Φ is defined and is C^r in both variables on a neighborhood of $(0, x_0) \in \mathbb{R} \times \mathbb{R}^n$.

If in components the function f is $f = (f_1, ..., f_n)$ then naturally associated to system (1) is the smooth vector field

$$X = f_1 \frac{\partial}{\partial x_1} + ... + f_n \frac{\partial}{\partial x_n} \tag{2}$$

on E. Then the solution curves of (1) are flow lines of X: the vector placed by X at a point $x_0 = \Phi(0, x_0)$ is the tangent vector $\Phi'(0, x_0)$ at x_0 of the solution curve $t \to \Phi(t, x_0)$ of (1). In the sequel we will use the same notation $f = (f_1, ..., f_n)$ for both the mapping in (1) and the corresponding vector field (2). Although many of the concepts discussed in this thesis hold for arbitrary n, henceforth we restrict to the case $n = 2$: two-dimensional systems. Such systems have wide applicability, yet are

especially amenable to study because orbits, as defined in Definition 1 which follows next, locally divide space.

In the following definition it is understood that values of t are restricted to the maximum interval of existence I of the solution through p.

Definition 1. In the context of Theorem 1, let $p \in E$. The orbit of (1) through p is the set $O(p) = \{\Phi(t, p) : t \in I\}$. The positive semi-orbit of (1) through p is the set $O_+(p) = \{\Phi(t, p) : t \geq 0\}$. The negative semi-orbit or (1) through p is the set $O_-(p) = \{\Phi(t, p) : t \leq 0\}$.

Definition 2. A point $x_0 \in \mathbb{R}^n$ is called a critical point of $\dot{x} = f(x)$ if $f(x_0) = 0$.

If we consider the geometric representation of a velocity vector field, then a critical point is one where the velocity vector is zero. Thus, the point itself is a trajectory. That is, if x_0 is a critical point of $\dot{x} = f(x)$ and $\Phi_t : E \to \mathbb{R}^n$ is the flow of the differential equation $\dot{x} = f(x)$, then $\Phi_t(x_0) = x_0$ for all $t \in \mathbb{R}$. A critical point x_0 of (1) is called a fixed point of the flow.

1.3 Phase Portrait

There are a few things we should note about Theorem 1 before we get started. First of all, we can see that $\mathbb{R}^n$ can be decomposed as a union of disjoint solution curves. For by the theorem any two solution curves must either agree everywhere or are disjoint from one another. When we assemble all of these solution curves together to form a union of disjoint curves, it forms the entire space $E \subset \mathbb{R}^2$. Lastly, we can conclude that, based on the theorem, each solution curve is, topologically, either a point, line, or an oval. These facts lead to the following fundamental definition.

Definition 3. The phase portrait of a system of ordinary differential equations with $x \in \mathbb{R}^2$ is the set of all solution curves in the phase space $\mathbb{R}^2$.

In Theorem 1 the mapping f will also be viewed as a vector field on $\mathbb{R}^2$. To get a rough idea of the nature of the phase portrait, we will first construct a direction field. A direction field is a popular method for displaying the general behavior of solution curves because it does not require a person to actually solve the differential equation. The direction field is a graph in which each point on the graph contains a line segment that corresponds with the tangent line of the solution. The line segment has an arrow placed at each point by f to show the direction of the tangent. In Figure 1 we see the direction field for the following example:

Example 1. Let $E = \mathbb{R}^2,\ f(x, y) = (2x, -3y)$. Thus,

$$\begin{aligned} \dot{x} &= \quad 2x \\ \dot{y} &= -3y. \end{aligned} \tag{3}$$

In Figure 1 we see the direction field of equation (3). Since the $\dot{x}$ and $\dot{y}$ are uncoupled we can solve each ode separately. Suppose that at time $t = 0$ the solution is at the point (x_0, y_0). The unique solution of the IVP is $\Phi(t, (x_0, y_0)) = (x_0 e^{2t}, y_0 e^{-3t})$ and $I((x_0, y_0)) = \mathbb{R}$. Choosing various specific starting points (x_0, y_0) we obtain Figure 2.

Similar to the direction field, a phase portrait is a visual representation of the solutions of a system of differential equations. By choosing various points of the phase plane as initial points we will then obtain a rough idea of the phase portrait of the system. To understand the phase portrait, one must first look at the flow of an ordinary differential equation. For this, we will use the parameters set up previously

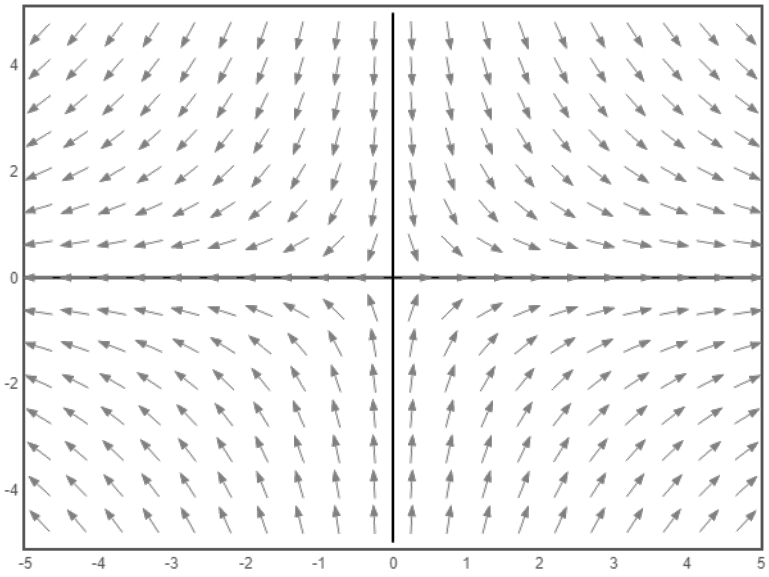

Figure 1: The Directional Field of Example 1

in Theorem 1. When (x_0, y_0) is fixed, $\Phi(t, (x_0, y_0))$ gives a curve in domain $f \subset \mathbb{R}^2$. All of these curves are the phase portrait.

Example 2. An example that illustrates the phase portrait well is the damped, unforced pendulum. In physics, the formula for the motion of the pendulum is derived from Newton's Second Law of Motion. Using this law, one obtains the second order ordinary differential equation given by (4) below, where m is the mass of the pendulum bob, c is the coefficient of friction, which is assumed proportional to linear velocity of the bob, ℓ is the length of the arm of the pendulum, assumed to be rigid and of negligible mass, and θ is the angle that the pendulum arm makes with the vertical (see Figure 3):

$$m\ell^2\ddot{\theta} + c\ell\dot{\theta} + mg\ell\sin\theta = 0 \tag{4}$$

where $c \geq 0$, and $m > 0$. We can simplify (4) by making $C = \frac{c}{m\ell}$ and $K = \frac{g}{\ell}$ where

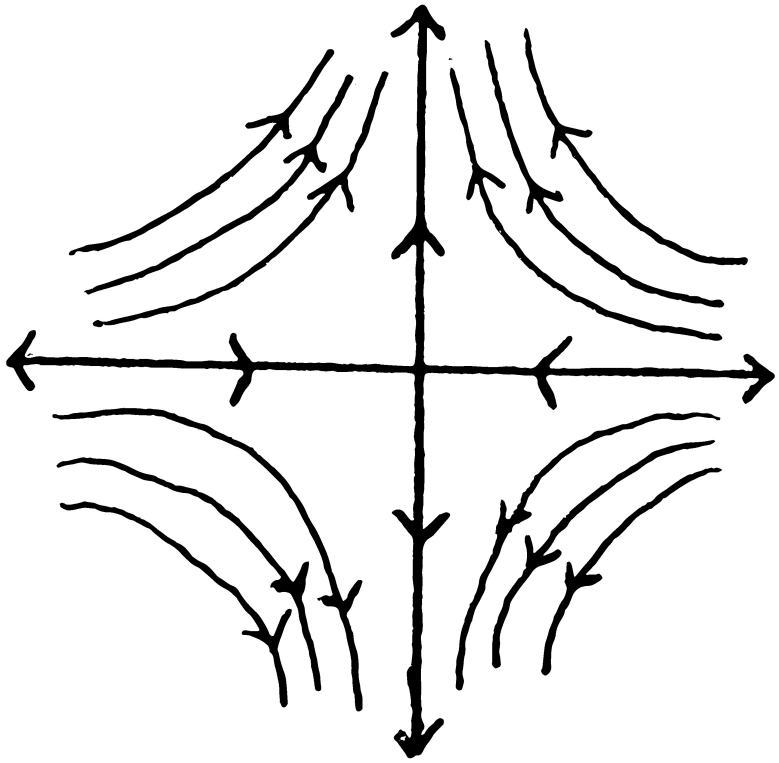

Figure 2: The Phase Portrait of Example 1

$C \geq 0$ and $K > 0$. Thus,

$$\ddot{\theta} + C\dot{\theta} + K \sin\theta = 0. \tag{5}$$

Now let us make this into a system of first order equations by introducing a second dependent variable ω defined by $\omega = \dot{\theta}$. Then

$$\begin{cases} \dot{\theta} = \omega \\ \\ \dot{\omega} = -C\omega - K\sin\theta \end{cases} \qquad C \geq 0, \quad K > 0 \tag{6}$$

The fixed points are easily found by setting the right hand sides in (6) equal to zero. Hence,

$$\dot{\theta} = \omega = 0 \Leftrightarrow \omega = 0$$

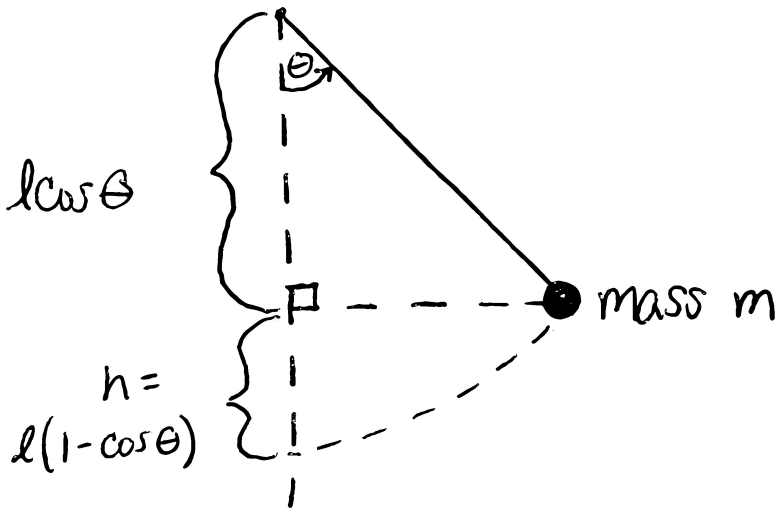

Figure 3: The Damped, Unforced Pendulum for Example 2

in which case

$$\dot{\omega} = -K \sin\theta = 0 \Leftrightarrow \theta = n\pi, n \in \mathbb{Z}.$$

Now, consider the total energy function. The total energy function can be written as $E =$ Potential Energy (PE) + Kinetic Energy (KE) and is

$$E = PE + KE = mgh + \frac{1}{2}mv^2$$

Using the ideas illustrated in Figure 3, we obtain

$$E = mgh + \frac{1}{2}mv^2 = mg\ell(1 - \cos\theta) + \frac{1}{2}m\ell^2\omega^2$$

Now, take the derivative with respect to t,

$$\frac{dE}{dt} = (mg\ell \sin\theta)(\dot{\theta}) + (m\ell^2\omega)(\dot{\omega}).$$

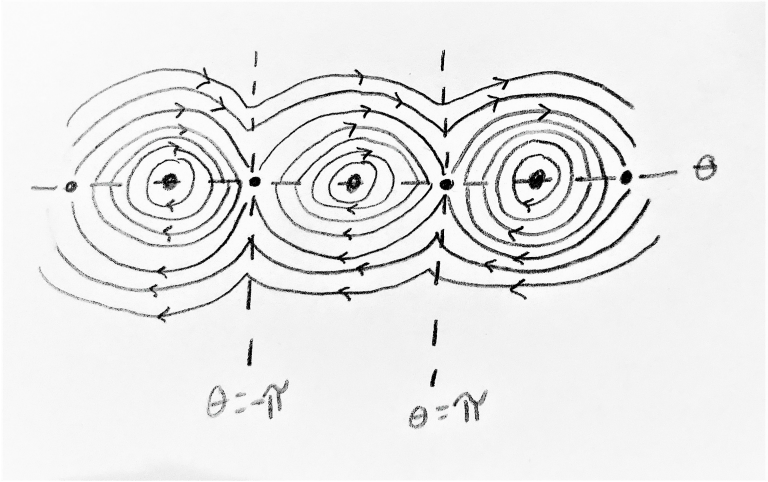

Figure 4: The Phase Portrait for Example 2

By equation (6),

$$\frac{dE}{dt} = (mg\ell \sin\theta)(\omega) + (m\ell^2\omega)(-C\omega - K\sin\theta)$$

Substituting back in $C = \frac{c}{m\ell}$ and $K = \frac{g}{\ell}$, we get

$$\begin{aligned}\frac{dE}{dt} &= (mg\ell \sin\theta)(\omega) + (m\ell^2\omega)(-\frac{c}{m\ell}\omega - \frac{g}{\ell}\sin\theta) \\ &= \omega mg\ell \sin\theta - cl\omega^2 - \omega mg\ell \sin\theta \\ &= -c\ell\omega^2\end{aligned}$$

In the idealized frictionless situation $c = 0$, in which case $\frac{dE}{dt} = 0$. In this case, the total energy is constant in time, hence trajectories lie in level curves of E. These level curves can be found algebraically. Using f to place arrows on the level curves, we obtain Figure 4, which illustrates the phase portrait of system (6) in the frictionless case $c = 0$.

The mathematical system (6) models the behavior of the physical system. Even though the mathematical system cannot be explicitly solved in closed form, the phase

portrait gives a full understanding of the behavior of this physical system in this special (ideal) case.

1.4 Periodic Solutions

By referencing back to the pendulum example, we can see the existence of orbits that are ovals or closed orbits. These closed orbits are representative of periodic motion in the idealized physical system.

Definition 4. Suppose that $x = \Phi(t)$ is a solution of the equation $\dot{x} = f(x)$, $x \in E \subset \mathbb{R}^2$ and suppose there exists a positive number T such that $\Phi(t+T) = \Phi(t)$ for all $t \in \mathbb{R}$. Then $\Phi(t)$ is called a periodic solution of the equation with period T. Periodic solutions are also known as periodic orbits or cycles.

Remark 1. If $\Phi(t)$ has period T, then by Definition 4 $\Phi(t+T) = \Phi(t)$. Thus $\Phi(t+2T) = \Phi(t+T+T) = \Phi(t+T) = \Phi(t)$. Thus, if $\Phi(t)$ has period T, it also has period $nT, \quad n \geq 1$.

Example 3. (Volterra-Lotka Model) The Volterra-Lotka Model is a predator-prey equation derived by Alfred Lotka and Vito Volterra independently. Volterra derived system (7) to model observed oscillatory levels of fish catches in the Adriatic Sea in 1925. The notion came from a marine biologist, Umberto D'Ancona, who would later become his son-in-law. D'Ancona noticed that the percentage of predatory fish had increased during World War I. Just slightly prior to Volterra's findings, Alfred Lotka independently formulated the same system of equations in 1920 to explain oscillatory behavior of the concentrations of two chemicals in a chemical reaction. Lotka later presented the same system in a biological context in 1926.

The system fails to consider any outside factors that may affect the predator and prey population. Thus, it is not entirely accurate in the real world and has never been successfully applied to any real-world data. For this reason, the system is of historical rather than practical importance. Attempts to develop it into a working model were an impetus to continued research in mathematical modelling of biological phenomena.

This system was formulated to describe the pattern of predators and prey and their effects on one another. The system derived by Lotka and Volterra can be written as

$$\begin{aligned} \dot{x} &= x(a - by) \\ \dot{y} &= y(dx - c) \end{aligned} \tag{7}$$

with $x, y \geq 0$ and a, b, c, d positive constants. Here, x denotes the population density of the prey. Likewise, y denotes the population density of the predator. In the prey equation, we can see that in the absence of predators, $y(0) = 0$, the density of the prey grows at a constant rate a. Similarly, in the absence of prey, $x(0) = 0$, the density of the predators decrease at a constant rate. However, in the presence of prey, the predators increase at a rate proportional to the density of the prey. To obtain a representation of the solutions of (7) for $x > 0$, $y > 0$, and $y \neq \frac{a}{b}$, by the chain rule we can write (7) as

$$\frac{dy}{dx} = \frac{y(dx - c)}{x(a - by)}.$$

Separating variables and integrating

$$\int \frac{a-by}{y}dy = \int \frac{dx-c}{x}dx$$

$$a\log y - by = dx - c\log x + K$$

$$dx - c\log x - by + a\log y = -K$$

so, the function

$$H : \{(x,y) : x > 0 \text{ and } y > 0\} \subset \mathbb{R}^2 \to \mathbb{R}$$

defined by

$$H(x,y) = dx - c\log x - by + a\log y$$

is constant on orbits of (7). We can see that the coordinate axes are invariant and by putting it all together we are able to draw the phase portrait (see Figure 5).

Looking at the phase portrait of Figure 5 we can deduce a few key ideas that will help us to better understand the system. In this graph, the x-axis is representative of the prey while the y-axis represents the predator volume (as stated above). In the phase portrait we can easily see exactly two critical points: the origin, and a unique critical point in the open first quadrant: $(\frac{c}{d}, \frac{a}{b})$. Also, notice that every other trajectory in the open first quadrant is an oval surrounding the critical point. Because this critical point is surrounded by cycles, it is referred to as a "center".

While this example is an idealized model, it does seem to match actual real world behavior to an extent. This is due to the fact that the populations that Lotka and Volterra were modeling actually do show periodic behavior like that of the mathematical system. A numerical plot of x and y as functions of t for a specific choice of

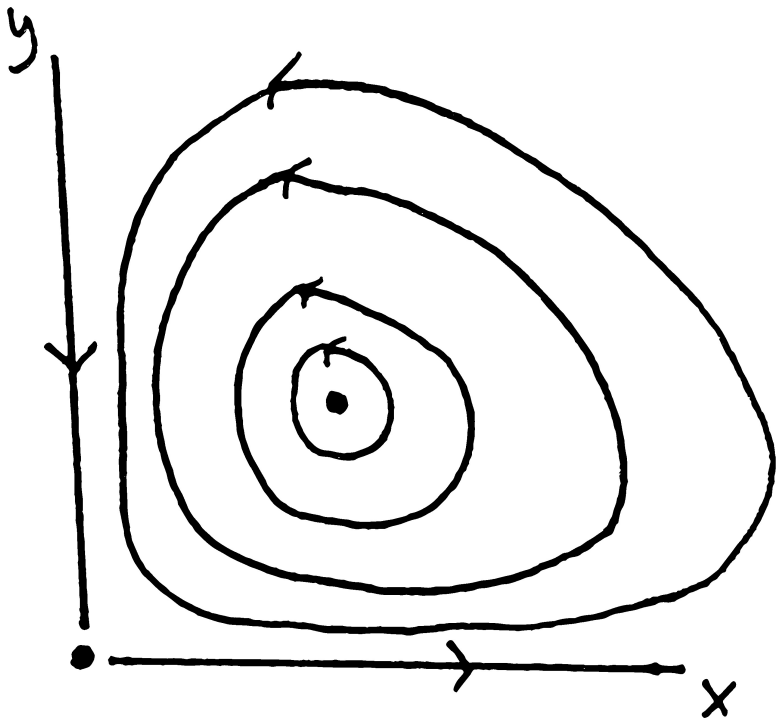

Figure 5: The Phase Portrait for the Volterra-Lotka System

the parameters a, b, c, and d is shown in Figure 6.

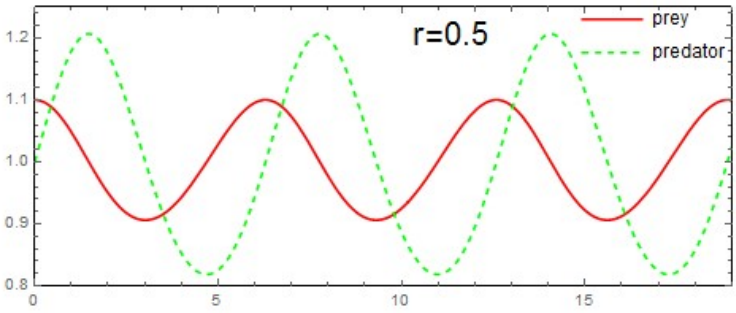

Figure 6: The Volterra-Lotka Model Predator Prey Graph

CHAPTER 2: BASIC IDEAS

2.1 Limit Cycles

In the 19th century, the great French mathematician Henri Poincaré made groundbreaking strides in the geometric analysis of systems of ordinary differential equations in two variables. With his study of systems of first order differential equations on the plane, Poincaré identified as of fundamental importance the existence of periodic orbits in phase portraits that are isolated from all other periodic orbits. He termed these orbits "cycles limites" [9], work extended fifteen years later by Ivar Bendixson [1].

Definition 5. A limit cycle is a cycle γ that is isolated from all other cycles in the sense that there exists a neighborhood U of γ which does not wholly contain any cycle besides γ.

Theorem 2. For real analytic systems, every cycle is either a limit cycle or a cycle in a "period annulus:" a band of concentric cycles that full up an annulus.

An example of the second case is the open first quadrant punctured at the critical point in the Volterra-Lotka system, Figure 5.

Proof of Theorem 2. The key idea in the proof, which goes back to Poincaré, is to construct a "local section" Σ of the flow at any point p on the cycle. This is a line segment through p that is perpendicular to $f(p)$ and so short that f is not tangent

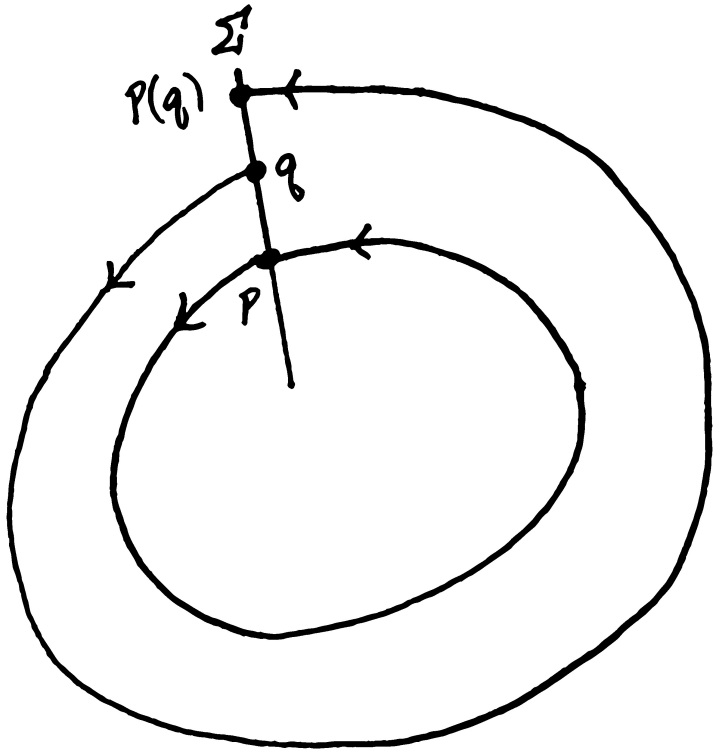

Figure 7: P Defined by a Neighborhood U of p

to Σ at any point. By means of the Implicit Function Theorem a "first return map" P is defined from a neighborhood U of p in Σ into Σ, as shown in Figure 7. It is real analytic, hence so is the difference map $d = P - id_\Sigma$. Cycles near p, at which d vanishes, are in one-to-one correspondence with zeros of d. Since d is analytic, if its zero at p is not isolated then $d \equiv 0$. □

We will need the following standard terminology. For simplicity, we make the non-essential assumption that the maximal interval of existence is $\mathbb{R}$.

Definition 6. In the context of Theorem 1, for $x_0 \in E$, the alpha limit set of x_0 and the omega limit set of x_0 are

$$\alpha(x_0) = \{x : \exists t_k, monotonic, t_k \to -\infty \text{ such that } \Phi(t_k, x_0) \to x\} \tag{8}$$

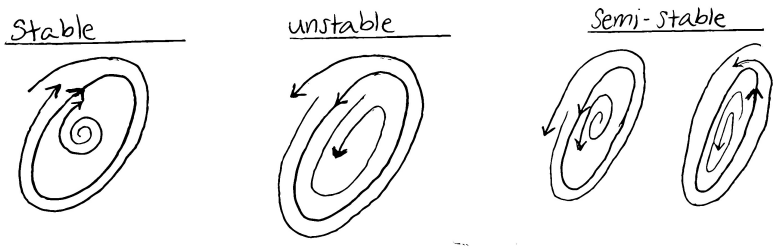

Figure 8: Examples of Stability for Definition 7

$$\omega(x_0) = \{x : \exists t_k, monotonic, t_k \to \infty \text{ such that } \Phi(t_k, x_0) \to x\} \tag{9}$$

Every point in the α-limit set of x_0 is called an α-limit point of x_0, and analogously for points in $\omega(x_0)$.

The following facts concerning α- and ω-limit sets will be needed.

Proposition 4. (a) If $O_+(p)$ (respectively $O_-(p)$) is confined to a compact set K, then the omega limit set $\omega(p)$ (respectively the alpha limit set $\alpha(p)$) is non-empty (and is a subset of K).

(b) $\omega(\omega(p)) \subset \omega(p)$ and $\alpha(\alpha(p)) \subset \alpha(p)$.

Poincaré proved that a limit cycle γ is the α- or ω-limit set of every point in a neighborhood of γ in the interior of γ (respectively, the exterior of γ) regarded as a simple closed point-set curve (see Theorem 3 below). This allows the following definition.

Definition 7. A limit cycle is termed stable if it is the ω-limit set of every point near it. A limit cycle is termed unstable if it is the α-limit set of every point near it. Lastly, a limit cycle is termed semi-stable if it is neither the α or ω limit set of every point near it (see Figure 8).

Stable limit cycles are of fundamental significance in systems of ordinary differential

equations that model real world phenomena because they correspond to periodic motion to which all nearby initial starting configurations tend asymptotically in future time. That is, these correspond to the periodic behavior of the system of the system to which all nearby starting configurations tend as time increases without bound.

Proving the existence and non-existence of limit cycles in real systems and locating them when they exist is a difficult problem. The following simple example is given in Perko [8]. It is an artificial example of a system that contains a limit cycle.

Example 5. Consider the system

$$\begin{aligned} \dot{x} &= -y + x(1 - x^2 - y^2) \\ \dot{y} &= x + y(1 - x^2 - y^2). \end{aligned} \tag{10}$$

Using the easily derived relationship between polar and rectangular coordinates $r\dot{r} = x\dot{x} + y\dot{y}$ and $r^2\dot{\theta} = x\dot{y} - y\dot{x}$, we have that in polar coordinates (10) is

$$\begin{aligned} \dot{r} &= r(1 - r^2) \\ \dot{\theta} &= 1 \end{aligned} \tag{11}$$

Since $\dot{r} = 0$ at $r = 0$, the origin is a critical point of the system. Since $\dot{r} = 0$ at every point for which $r = 1$, the unit circle is an invariant set for the flow, and since it contains no critical point, it is a closed orbit. Furthermore, for $0 < r < 1$ we see that the flow spirals outward since $\dot{r} > 0$. Likewise, for $r > 1$ we see that the flow spirals inward since $\dot{r} < 0$ for all $r > 1$. Thus, the unit circle is a stable limit cycle.

CHAPTER 3: EXISTENCE AND NON-EXISTENCE OF LIMIT CYCLES

Let us first look at the phase portraits for examples that we have already done. You'll notice that in all of our examples, every cycle goes around a critical point of the system. This is a result that is true in general, and is proved using the theory of index of critical points and of vector fields along simple closed curves, which we will now develop.

3.1 Index

In our discussion of index, our arguments will be for the most part intuitive to a large degree, avoiding technicalities.

We will make the following assumptions throughout this section: We suppose we are in the situation of Theorem 1: $E \subset \mathbb{R}^2$ is an open set and $f : E \to \mathbb{R}^2$ is a C^r mapping, $r \geq 1$, which will be viewed as a vector field on E. Cycles and critical points are those of the system $\dot{x} = f(x), x \in E$.

We will need the following general result. A closed curve (i.e., a point-set that is the topological image of the unit circle) is simple if it does not self-intersect. In particular, every cycle is a simple closed curve.

Theorem 3 (Jordan Curve Theorem). The complement of a simple closed curve C in the plane is the union of two disjoint, open, path-connected sets, one of them bounded, the other unbounded. The bounded component of the complement is called

the interior of C, denoted $Int(C)$; the unbounded component of the complement is called the exterior of C, denoted $Ext(C)$.

Remark 2. The Jordan Curve Theorem is not true on every surface. For example, the Jordan Curve Theorem fails to hold true on a torus.

We alert the reader to the fact that for the next few paragraphs (as far as Theorem 5, below) the simple closed curves under discussion are arbitrary curves in E, and need not be cycles of the system $\dot{x} = f(x)$.

In order to avoid extended discussion using limit arguments based on the continuity of f, we will loosen our terminology and refer to a closed curve like that shown in Figure 12, defined as C_1 followed by arc L followed by $-C_2$ followed by $-L$ as a simple closed curve (where in a detailed argument in place of L we would have two very close and oppositely oriented parallel arcs and take a limit as they become arbitrarily close as point-sets).

Definition 8. The index of a simple closed curve C with respect to a continuous vector field f which is defined and non-zero everywhere on $C \subset E$ is the number $I_f(C)$ of complete counterclockwise revolutions of f as C is traversed one time counterclockwise.

Remark 3. If C is traversed clockwise, then the number of complete counterclockwise revolutions of f is $-I_f(C)$. We denote the clockwise traversal of C by $-C$, and thus we have $I_f(-C) = -I_f(C)$.

Proposition 6. If $f(p) \neq 0$ then for a sufficiently small circle C centered at p, $I_f(C) = 0$.

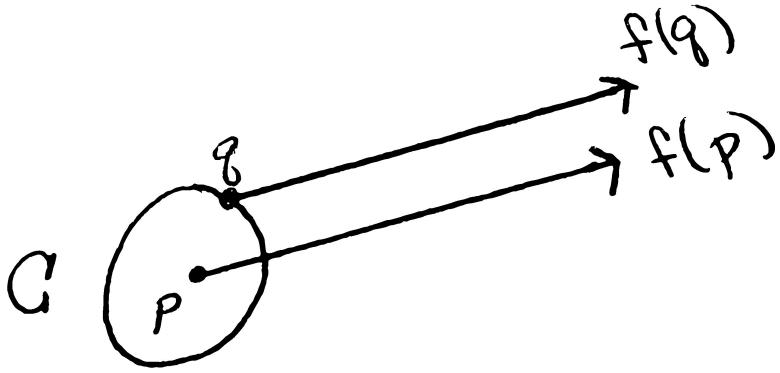

Figure 9: A Sufficiently Small Circle Centered at p in Proposition 6

Proof. By continuity of f there exists a neighborhood U of p such that at any point q in U the angle formed by the vectors $f(p)$ and $f(q)$ is less than (say) $\frac{\pi}{6}$. Then for any circle $C \subset U$ and centered at p it is clear that $f(q)$ makes zero revolutions as the point q traverses C once completely. □

Proposition 7. Suppose that for a simple closed curve C, f is defined and non-zero on $C \cup Int(C)$. Then $I_f(C) = 0$.

Proof. For a directed arc L, let $\Delta_f(L)$ denote the change in the angle that f makes when L is traversed from one end to the other. In analogy with Remark 3, $\Delta_f(-L) = -\Delta_f(L)$. Consider Figure 10, in which an arc L_1 in $Int(C)$ joins two points on C, forming two simple closed curves C_1 and C_2 as shown, each composed of L and an arc in C. Giving a counterclockwise orientation to each of C_1 and C_2 orients L_1 twice, but in opposite directions.

Clearly $I_f(C) = I_f(C_1) + I_f(C_2)$ by the cancellation in traversing L_1 in each direction. If we were to add a second arc L_2 similarly, but crossing L_1 at a single point,

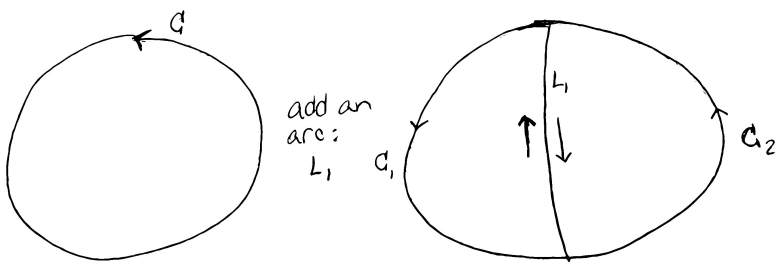

Figure 10: Adding an Arc L_1 to a Cycle

four simple closed curves would be formed. We can continue to add more and more arcs, resulting in an increasing number of smaller and smaller curves.

Figure 11 shows 20 small simple closed curves $C_1, ..., C_{20}$, and similarly since f is non-zero in $Int(C)$, $I_f(C_j)$ is defined for $1 \leq j \leq 20$ and $I_f(C) = I_f(C_1)+...+I_f(C_{20})$. Since there are no critical points in $Int(C)$ this process can be continued until all the small simple closed curves C_j are so small that Proposition 6 applies to each one, hence $I_f(C_j) = 0$ for all values of C_j, hence $I_f(C) = \sum I_f(C_j) = \sum 0 = 0$. □

Corollary 8. If C_1 and C_2 are Jordan curves contained in E with $C_2 \subset Int(C_1)$, $f(p) \neq 0$ for $p \in C_2 \cup [Ext(C_2) \cap Int(C_1)] \cup C_1$, then $I_f(C_2) = I_f(C_1)$.

In other words, if C_2 can expand out towards C_1 without crossing a single critical point of f, then the index of C_2 will be equal to the index of C_1.

Proof. To prove Corollary 8, refer to Figure 12. Choose a smooth arc L in $Int(C_1) \cap Ext(C_2)$ oriented from C_1 to C_2. We will start on the curve C_1. Follow this curve all the way around until it reaches L then follow L down to C_2. Next, follow $-C_2$ around until it reaches L. Lastly, we will follow $-L$ until it reaches C_1 to form a

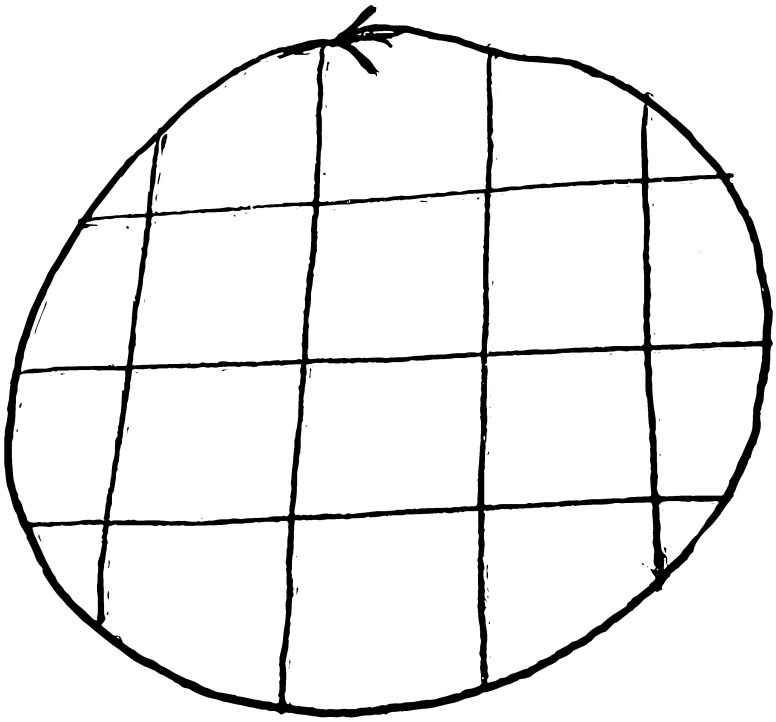

Figure 11: Multiple Arcs Added to a Cycle

closed curve. Now, by Remark 3 and Proposition 7

$$\begin{aligned} 0 &= I_f(C) \\ &= I_f(C_1) + \Delta_f(L_1) + I_f(-C_2) + \Delta_f(-L_1) \\ &= I_f(C_1) + \Delta_f(L_1) - I_f(C_2) - \Delta_f(L_1) \\ &= I_f(C_1) - I_f(C_2) \end{aligned}$$

This implies then that $I_f(C_1) = I_f(C_2)$. □

Corollary 8 allows the following definition:

Definition 9. For any $p \in E$, the index of p with respect to f is $I_f(p) = I_f(C)$ for any simple closed curve that contains no critical point of f on it or on its interior, except possibly for p.

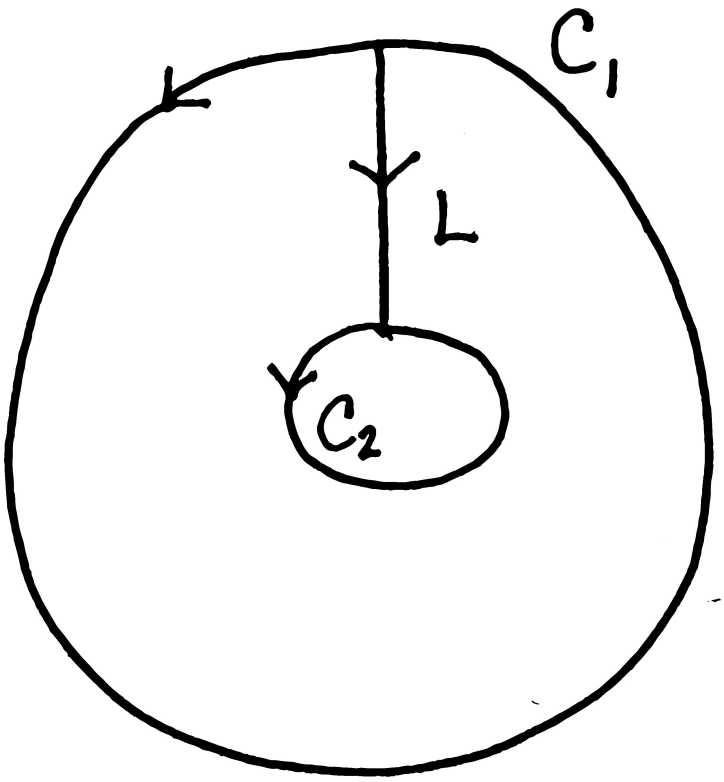

Figure 12: Adding an Arc L_1 to Two Cycles

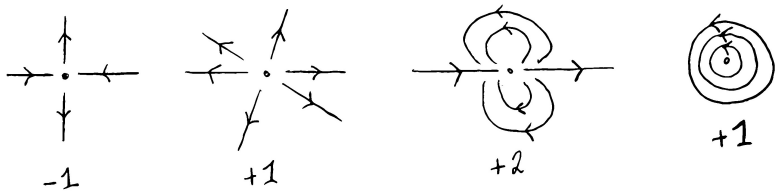

Figure 13: Examples of the Index for Four Critical Points

By Proposition 6, the index of any regular point p (point at which $f \neq 0$) is zero. The indices of four critical points of distinct "topological type" are shown in Figure 13. The following result will also be needed, but its proof is technical and not enlightening so we will omit it here.

Theorem 4 (Umlaufsatz). If γ is a cycle of f, hence a simple closed curve, and is positively oriented, then $I_f(\gamma) = +1$.

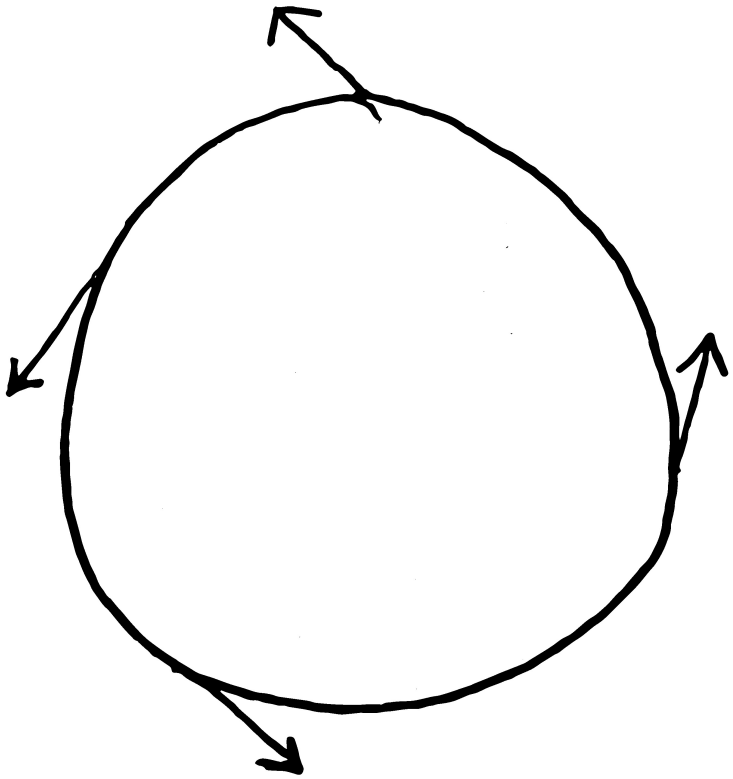

Figure 14: The Index of a Circle C

In reference to the Umlaufsatz (Theorem 4), refer to Figures 14, 15, and 16. Each figure shows a simple closed curve that is positively oriented. In Figure 14 it is obvious that the index of the circle is $+1$. In Figure 15, it becomes slightly more difficult to see that the index is $+1$. However, it is still very clear. In Figure 16, it becomes much more difficult to determine the index. While it is still reasonable to determine its index by sight alone, it is not as obvious as the other two that its index is also $+1$.

We now state and prove the main result of this section, the most important application of the theory of index to cycles of systems of the form (1) on the plane.

Theorem 5. If γ is a cycle of $\dot{x} = f(x)$ and f is defined on $\gamma \cup Int(\gamma)$, then there must exist a critical point of f in $Int(\gamma)$.

Proof. Reverse all vectors by replacing f by $-f$ if necessary so that γ is positively

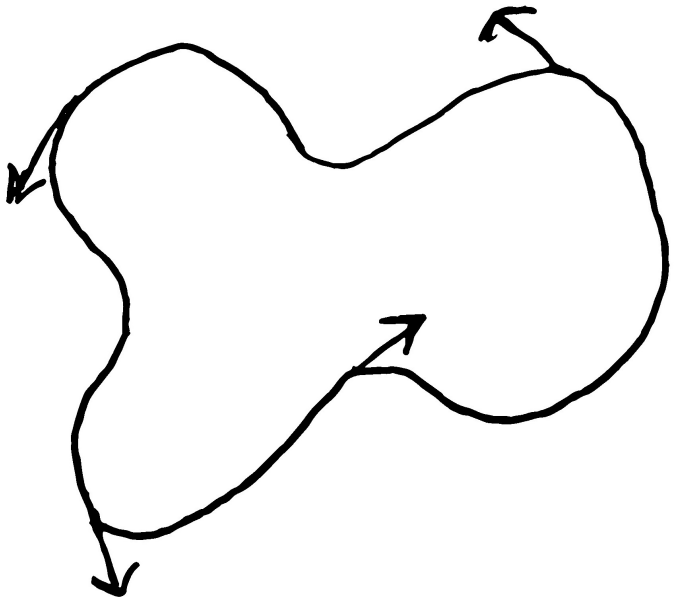

Figure 15: The Index of a Simple Closed Curve C

oriented. Contrary to what we wish to show, suppose that there are no critical points in $Int(\gamma)$. Then by Proposition 7 the index $I_f(\gamma)$ is zero. However, by Theorem 4, $I_f(\gamma)$ must be $+1$. Thus, we have a contradiction and have proved that there is at least one critical point in $Int(\gamma)$. □

A slight extension of Theorem 5 is the following

Theorem 6. If the number of critical points of f in $Int(\gamma)$ is finite then their indices sum to 1.

Proof. The idea of the proof is contained in Figure 17, shown in the case that there are three critical points in $Int(\gamma)$. Since they are finite in number, they can be isolated from one another by three small positively oriented circles C_1, C_2, and C_3, as

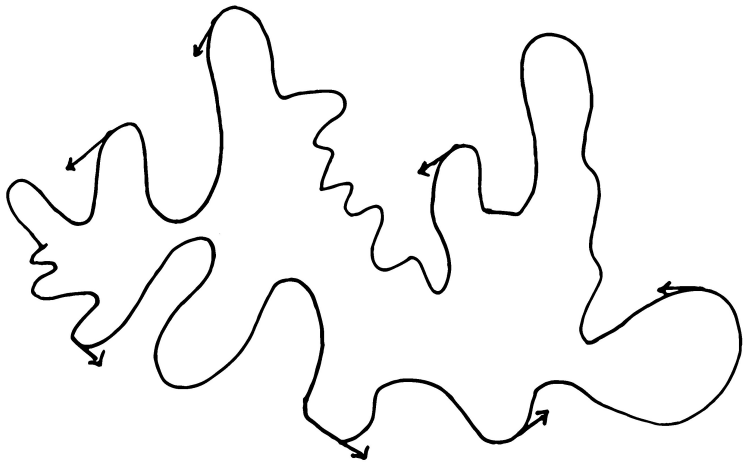

Figure 16: The Index of a Simple Closed Curve C

shown. The circles in turn can be joined by two oriented arcs L_{12} and L_{23}, as shown. Reversing the flow if necessary so that γ is positively oriented, the index of the curve made up of the shrinking down of γ onto $C_1 \cup L_{12} \cup C_2 \cup L_{23} \cup C_3$ is that of γ, namely $+1$, but is also $\sum I_f(C_j)$, since the contributions of L_{12} and L_{23} cancel, since they are traversed twice in opposite directions. □

3.2 Poincaré-Bendixson Theorem

One of the most important theorems in the theory of cycles of systems of the form (1) on the plane is the following.

Theorem 7. (Poincaré-Bendixson Theorem) Suppose that:

1) R is a closed, bounded subset of the plane;

2) $\dot{x} = f(x)$ is a continuously differentiable vector field on an open set containing R;

3) p is a point in R such that $O_+(p) \subset R$.

Then the ω-limit set of p is non-empty by Proposition 4 and either contains a critical point (in R) or is a closed orbit (confined to R). Similarly for the alpha limit set if

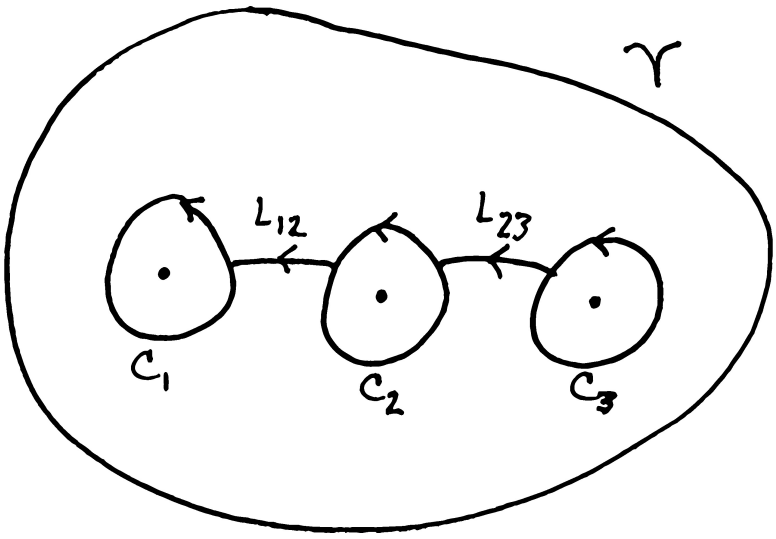

Figure 17: The Image of The Proof of Theorem 6

$O_-(p) \subset R$.

Remark 4. If the system of (1) is real analytic, then the closed orbit in question must be a limit cycle, since by Theorem 2 a picture like Figure 18, or a sequence of cycles isolated from one another collapsing onto a particular cycle, is impossible for real analytic systems.

Proof. The proof of the Poincaré-Bendixson Theorem depends in an essential way on the Jordan Curve Theorem (Theorem 3) and the Flowbox Theorem (which states that the flow in a neighborhood of a regular point is smoothly equivalent to the flow of the system $\dot{x} \equiv 1$, $\dot{y} \equiv 0$). A sketch of the proof is as follows. If $\omega(p)$ contains a critical point then there is nothing to show. Otherwise, since by Proposition 4 (a) $\omega(p) \neq \varnothing$, we select any point $q \in \omega(p)$, erect a section Σ of the flow at q and build

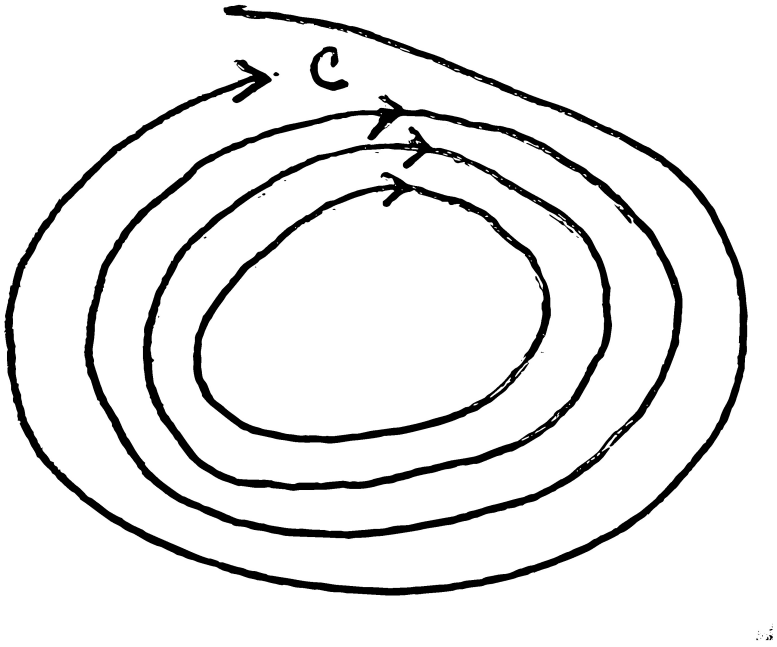

Figure 18: A Band of Cycles Inside of C

a flowbox on it. Then there must exist a sequence of times $t_k \to \infty$ monotonically such that $p_k = \Phi(t_k, p)$ is a sequence in Σ that tends monotonically to q. For as Figure 19 suggests (the rigorous derivation is much more elaborate) the solution arc $\{\Phi(t,p) : t_k \leq t \leq t_{k+1}\}$ together with the segment $[p_k, p_{k+1}]$ of Σ form a simple closed curve C, and $O_+(p_{k+1})$ is on the same side (either $Int(C)$ or $Ext(C)$) as q, and that side is positively invariant. Certainly $O_+(q) \subset R$, else continuity of solutions in initial conditions and convergence of the sequence (p_k) to q would imply that $O_+(p) \not\subset R$, which is false.

But then, by Proposition 4 (a), $\omega(q) \neq \varnothing$, so we may select any $q' \in \omega(q) \subset \omega(p)$ (Proposition 4 (b)) and erect a section Σ' of the flow at q' and build a flowbox on it.

There is a sequence $t'_j \to +\infty$ monotonically such that $q_j = \Phi(t'_j, q) \in \Sigma'$ tends

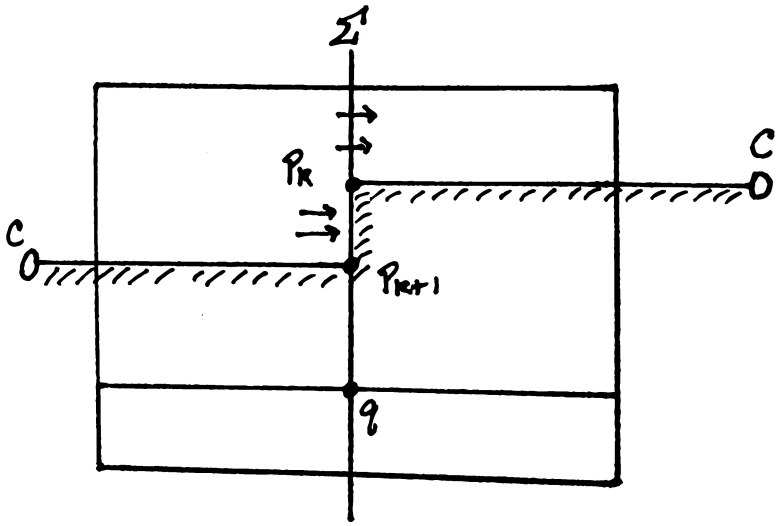

Figure 19: The Shaded Positively Invariant Side of C

monotonically to q'.

If $q_j = q'$ for any j then q is a periodic point (i.e., the orbit $O(q)$ is a cycle), as required. Otherwise, fixing any $j \in \mathbb{Z}^+$, let C' denote the simple closed curve formed by the solution arc $\{\Phi(t, q_j) : t'_j \leq t \leq t'_{j+1}\}$ and the segment $[q_j, q_{j+1}]$ of Σ' (see Figure 20). Let $Side_1(C')$ be the positively invariant side of C' (either $Int(C')$ or $Ext(C')$, it does not matter for the argument which); $O_+(q_{j+1}) \subset Side_1(C')$ but $q \in Side_2(C')$. Choose k so large that p_k is so close to q that (recalling that $q_{j+1} = \Phi(t'_{j+1}, q)$) $\Phi(t'_{j+1}, p_k)$ is in the flowbox enclosing q', which implies that $O_+(p_k)$ must enter $Side_1(C')$ along with $O_+(q_{j+1})$. But then $\Phi(t, p) \in Side_1(C')$ for $t > t_k + t'_{j+1} + 1$, which means it cannot again approach q, which is false. □

We remark in passing that there are versions of the Poincaré-Bendixson Theorem

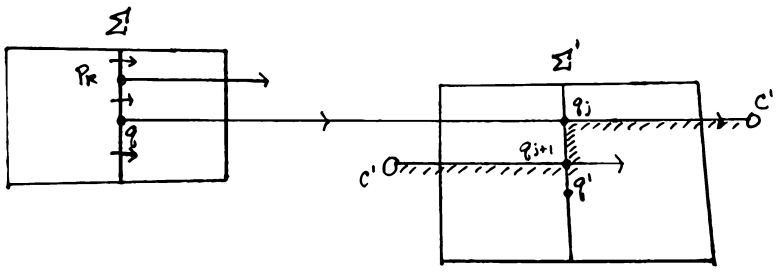

Figure 20: The Shaded Positively Invariant Side of C'

with more detailed conclusions, in particular concerning the nature of $\omega(p)$ when it contains a critical point. The version presented here addresses all the issues needed insofar as applicability to the existence of limit cycles is concerned.

We also note that all these versions hold true for vector fields on the 2-sphere S^2, on which the Jordan Curve Theorem is also valid (except, of course, for boundedness and unboundedness to distinguish components of the complement of C), but do not hold for surfaces in general. For example, for the irrational flow on the 2-torus T^2, obtained from the system $\dot{x} \equiv 1$, $\dot{y} \equiv m$, m irrational, on $\mathbb{R}^2$ by identifying opposite sides of the unit square, for any $p \in T^2$, $\omega(p)$ is all of T^2.

3.3 Poincaré Annular Region Theorem

The following theorem is of great practical use in proving existence of closed orbits.

Theorem 8. (Poincaré Annular Region Theorem) Suppose A is the diffeomorphic image of the annulus

$$\{(x, y) : 1 \leq x^2 + y^2 \leq 2\}$$

and that f is a C^1 vector field on a neighborhood of A with the following properties:
(1) f points into A (respectively, out of A) at every point of the boundary ∂A of A; and
(2) f has no critical points in A.
Then $\dot{x} = f(x)$ has a cycle that is wholly contained in the interior of A.

Proof. Suppose that A and f are as in Theorem 8 and fix $p \in \partial A$. By Theorem 7, $\omega(p) \neq \varnothing$ and either contains a critical point or is a closed orbit. However, by the hypothesis, there is no critical point in A. Hence, $\omega(p)$ must be a closed orbit in A. □

Note that by Theorem 5 the closed orbit guaranteed by Theorem 8 to exist must "go around the hole" in A.

3.4 Bendixson's Criterion

Bendixson's Criterion is a key tool for proving the non-existence of closed orbits in particular systems. It was formulated by Swedish mathematician Ivar Bendixson in 1901.

Definition 10. A set $E \subset \mathbb{R}^2$ is simply connected if every simple closed curve in E can be shrunk in E to a point in E.

Theorem 9. Suppose $E \subset \mathbb{R}^2$ is a simply connected open set and $f : E \to \mathbb{R}^2$ is a C^r

mapping, $r \geq 1$. If $div(f) := \frac{\partial f}{\partial x} + \frac{\partial f}{\partial y} : E \to \mathbb{R}$ is of one sign in E, and not identically zero on E, then there are no cycles of $\dot{x} = f(x)$ that are wholly contained in E.

Proof. Theorem 9 is a corollary of the somewhat more general version of the same result, Dulac's Criterion, Theorem 10, which we will prove below. □

Example 9. The system

$$\dot{x} = y^2 - x$$

$$\dot{y} = x^2 - y^3$$

has two singularities, a hyperbolic saddle at $(1, 1)$ and a non-hyperbolic singularity at $(0, 0)$. The behavior on the isoclines makes it look like there are no cycles. In fact,

$$div(f(x, y)) = \frac{\partial}{\partial x}(y^2 - x) + \frac{\partial}{\partial y}(x^2 - y^3) = -1 - 3y^2 \leq -1 < 0.$$

By Bendixson's Criterion, there cannot be a cycle.

3.5 Dulac's Criterion

An extension of Bendixson's Criterion is Dulac's Criterion. Since Bendixson's Criterion was formulated before Dulac's Criterion we stated Bendixson's Criterion first.

Theorem 10. Suppose $E \subset \mathbb{R}^2$ is a simply connected open set, $f : E \to \mathbb{R}^2$ and $B : E \to \mathbb{R}$ are C^r, $\quad r \geq 1$, and $div(Bf) \not\equiv 0$ and is of one sign on E. Then no closed orbit of $\dot{x} = f(x)$ lies wholly within E.

Proof. Suppose E, f, and B are as stated except for any conditions on $div(Bf)$, and let γ be a closed orbit of $\dot{x} = f(x)$ in E which we may assume without loss of generality

is positively oriented as a solution curve of $\dot{x} = f(x)$. Writing $f = (p, q)$,

$$\begin{aligned} I &= \int\int_{Int(\gamma)} div(Bf)\, dA \\ &= \int\int_{Int(\gamma)} \frac{\partial}{\partial x}(Bp) + \frac{\partial}{\partial y}(Bq)\, dA \\ &= \int\int_{Int(\gamma)} \frac{\partial}{\partial x}(Bp) - \frac{\partial}{\partial y}(-Bq)\, dA \end{aligned}$$

Using Green's Theorem, $\int_C P dx + Q\, dy = \int\int_{int(C)} Q_x - P_y\, dA$,

$$I = \int_\gamma -Bq dx + Bp\, dy$$

Parametrizing γ by any solution of (1), $\gamma = (x(t), y(t))$ on $[0, T], dx = \dot{x}(t)dt = p(x(t), y(t))dt$ and $dy = \dot{y}(t)dt = q(x(t), y(t))dt$, hence

$$\begin{aligned} I &= \int_0^T (-Bqp)(x(t), y(t)) + (Bpq)(x(t), y(t))dt \\ &= \int_0^T 0\, dt \\ &= 0. \end{aligned}$$

Therefore, either $div(Bf) \equiv 0$ on E or $div(Bf)$ changes sign on E. □

Example 10. Consider the system

$$\dot{x} = 1 - y^2$$

$$\dot{y} = xy + y^3$$

We can check that the only singularities are hyperbolic nodes or foci located at $(-1, \pm 1)$. They are in fact foci (see Perko's Example 5 in Section 4.1 [8]). Since y factors out of the $\dot{y}$ equation, the x-axis $y = 0$ is an invariant line. Thus, any cycle must either lie wholly in the upper half plane $y > 0$ or wholly in the lower half plane

$y < 0$ and enclose one of the singularities. To try to prove non-existence of any closed orbits we will first try Bendixson's Criterion. We compute

$$div(f(x,y)) = \frac{\partial}{\partial x}(1-y^2) + \frac{\partial}{\partial y}(xy+y^3) = 0 + x + 3y^2$$

which vanishes along the curve $x = -3y^2$. Thus, Bendixson's Criterion is inconclusive.

Next, let us look for a Dulac function of the form $B(x,y) = y^p$. We compute

$$\begin{aligned} div(Bf) &= \frac{\partial}{\partial x}(y^p - y^{p+2}) + \frac{\partial}{\partial y}(xy^{p+1} + y^{p+3}) \\ &= 0 + (p+1)xy^p + (p+3)y^{p+2} \\ &= y^p[(p+1)x + (p+3)y^2] \end{aligned}$$

which vanishes along $y = 0$ (for $p > 0$) and along the curve C_p: $x = -\frac{p+3}{p+1}y^2$ (for $p \neq -1$).

If E_p is the shaded region of Figure 21 then by Dulac's Criterion there is no cycle within E_p throughout which $div(Bf)$ is of one sign. However, the upper half plane is equal to $\{(x,y) : y > 0\} = \cup_{p>-1} E_p$. Hence, there is no cycle in the upper half plane. Similarly there is none in the lower half plane. Hence, none at all.

Example 11. Now, consider the system

$$\dot{x} = 2xy$$

$$\dot{y} = 2xy - x^2 + y^2 + 1$$

The y-axis $x = 0$ is invariant. The critical points satisfy $\dot{x} = 0$. Hence $x = 0$ or $y = 0$. If $x = 0$ then $\dot{x} = y^2 + 1 > 0$. Thus there are no critical points there. However, if $y = 0$, then $\dot{y} = 1 - x^2$. Now the only critical points are $(-1, 0)$ and $(1, 0)$ which are a hyperbolic sink and source, respectively.

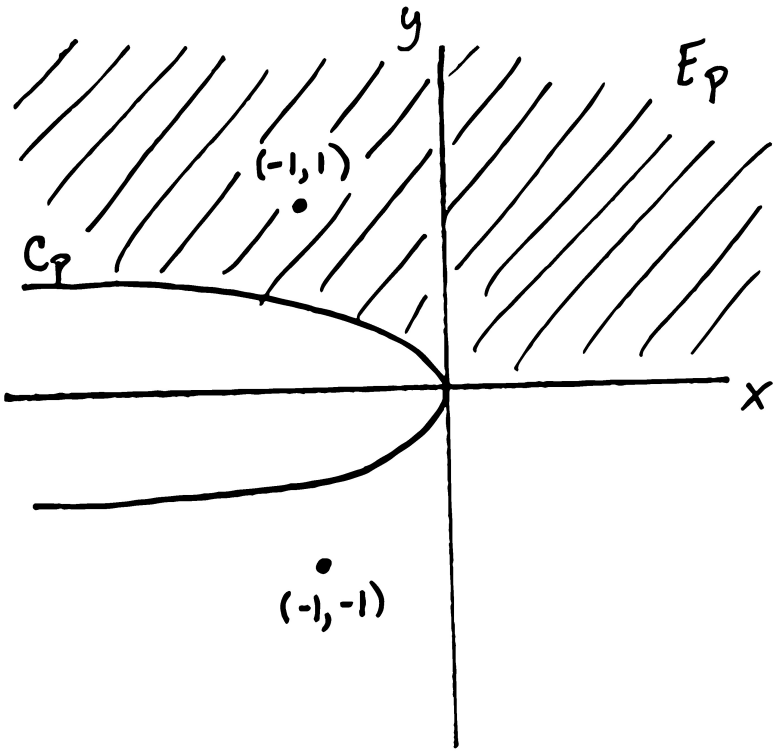

Figure 21: The Graph of The Dulac Function for Example 10

In the paper [3], it was necessary to show that there were no closed orbits. If there is a closed orbit then it must lie either completely within the right half plane $x > 0$ or completely within the left half plane $x < 0$. We will begin by trying to apply Bendixson's Criterion:

$$\begin{aligned} div f(x,y) &= \frac{\partial}{\partial x}(2xy) + \frac{\partial}{\partial y}(2xy - x^2 + y^2 + 1) \\ &= 2y + 2x + 2y \\ &= 2(x + 2y) \end{aligned}$$

which vanishes along the line $x + 2y = 0$ or $y = -\frac{1}{2}x$. Thus, it is inconclusive since it excludes "small" cycles surrounding the critical points, but not "large" ones.

Now, let us consider $B(x,y) = 2x^{-2}$ which exists on $\mathbb{R}^2 \setminus \{(x,y) : x = 0\}$. It satisfies

$$\begin{aligned} div(Bf) &= \frac{\partial}{\partial x}(4x^{-1}y) + \frac{\partial}{\partial y}(4x^{-1}y - 2 + 2x^{-2}y^2 + 2x^{-2}) \\ &= -4x^{-2}y + 4x^{-1} + 4x^{-2}y \\ &= 4x^{-1} \end{aligned}$$

which is not identically zero and is of one sign on the right half plane ($x > 0$). Hence, there are no cycles wholly contained in the right half plane. Similarly it is not identically zero and is of one sign on the left half plane. Thus, there are no cycles wholly contained in the left half plane. Therefore, there are no cycles at all.

A Dulac function and the ideas in Bendixson's Criterion can also be used to prove the following extension of Theorem 8, which will be applied to the van der Pol oscillator.

Theorem 11. If in the context of the Poincaré Annular Region Theorem, Theorem 8, there exists a C' function $B : Int(A) \to \mathbb{R}$ such that $div(Bf)$ is not identically zero on any open subset of $Int(A)$ and is of one sign on $Int(A)$, then the cycle in A is unique.

Proof. Suppose γ_1 and γ_2 are two cycles in A, which by hypothesis (2) in Theorem 8 and Theorem 5 must both surround the bounded subset of the complement of A, hence be nested, say with $\gamma_2 \subset Int(\gamma_1)$, and with the annular region A' that they bound a subset of A. Let C_1 and C_2 be the positively oriented simply closed curves that γ_1 and γ_2 form as point-sets (ignoring their orientation induced by the flow), and let L be a smooth oriented arc in A' joining C_1 and C_2 so the situation is as shown in Figure 12. Consider the simple closed curve $C \stackrel{\text{def}}{=} C_1 + L + (-C_2) + (-L)$. Applying

the same computations as were done in the proof of Dulac's Criterion, Theorem 10, we find that either $div(Bf) \equiv 0$ on the open set A' in A or $div(Bf)$ changes sign on $A' \subset A$. $\square$

CHAPTER 4: CYCLES IN AN IMPORTANT FAMILY

4.1 Liénard Systems

Systems of the form

$$\ddot{x} + f(x)\dot{x} + g(x) = 0 \tag{12}$$

were studied in the context of the existence of limit cycles in 1928 by French physicist Alfred Marie Liénard. They are now known as Liénard systems. In this section we will state and prove a theorem guaranteeing the existence of a stable limit cycle in the phase portrait of the system of two first order ordinary differential equations corresponding to (12), thereby yielding existence of asymptotically stable periodic solutions of (12).

In order to not break the flow of the proof of Liénard's Theorem we state and prove here a lemma that will be needed later.

Lemma 12. If, in the context of Theorem 1, a compact set $K \subset E$ is simply connected and contains no critical point, then for any point $p \in K$ both $O_+(p)$ and $O_-(p)$ exit K (i.e., $O_+(p) \not\subset K$ and $O_-(p) \not\subset K$).

Proof. Suppose, contrary to what we wish to show, that $O_+(p) \subset K$, which, because it is compact, is closed and bounded. By the Poincaré-Bendixson Theorem, Theorem 7, $\omega(p)$ either contains a critical point or is a closed orbit (contained in K). The former case is impossible, by the hypothesis that there is no critical point in K. But

the latter case is also impossible, for if γ were a closed orbit in K, then because K is simply connected f is defined on $\gamma \cup Int(\gamma)$. Hence, by Theorem 5 there would be a critical point in $Int(\gamma) \subset K$, contradicting the hypothesis that K contains no critical point. Thus, $O_+(p) \not\subset K$, as was to be shown. The conclusion for $O_-(p)$ follows simply by reversing the flow. □

Theorem 12. (Liénard's Theorem) Given $\ddot{x} + f(x)\dot{x} + g(x) = 0$, suppose

- f and g are C^r, $r \geq 1$,
- $xg(x) > 0$ for $x \neq 0$,
- f is such that the function F defined by $F(x) = \int_0^x f(u)du$ has two properties:

1) There exists constants $\alpha < 0 < \beta$ such that

a) $F(x) > 0$ if $\alpha < x < 0$

b) $F(x) < 0$ if $0 < x < \beta$.

2) a) $\lim_{x\to-\infty} F(x) = -\infty$,

b)$\lim_{x\to\infty} F(x) = +\infty$.

Then the phase portrait of (12) contains a closed orbit.

Remark 5. By the Fundamental Theorem of Calculus, F is differentiable with $F' = f$.

Proof of Theorem 12. From Equation (12), we get

$$-g(x) = \ddot{x} + f(x)\dot{x} = \frac{d}{dt}[\dot{x} + F(x)]$$

Rather than making (12) into an equivalent system the usual way (namely, introducing $y = \dot{x}$), we are lead to define the function $F(x) = \int_0^x f(s)ds$ of the statement of

the theorem and introduce the new variable $y = \dot{x} + F(x)$. Thus,

$$-g(x) = \frac{d}{dt}[\dot{x} + F(x)] = \frac{d}{dt}y = \dot{y}$$

Hence, we get

$$\begin{aligned} \dot{x} &= y - F(x) \\ \dot{y} &= -g(x) \end{aligned} \tag{13}$$

which is equivalent to (12). Since (12) and (13) are equivalent, it is enough to find a closed orbit in the phase portrait of (13).

Since $xg(x) > 0$ for $x \neq 0$, $g(x) > 0$ if $x > 0$ and $g(x) < 0$ if $x < 0$, hence by continuity of g, $g(x) = 0$ if and only if $x = 0$. Since $F(0) = 0$, $(x, y) = (0, 0)$ is the unique critical point of (13). Now introduce, in analogy with the pendulum example, an "energy" function:

$$V(x, y) = \frac{1}{2}y^2 + G(x), \tag{14}$$

where $G(x) = \int_0^x g(u)du$. Recall that g is continuously differentiable implying that $G(x)$ exists and is differentiable with $G'(x) = g(x)$. But then, by the properties of the function $g(x)$ just described, $G(x)$ is strictly decreasing for $x < 0$ and is strictly increasing for $x > 0$. Since $G(0) = 0$, it follows immediately from the definition of $V(x, y)$ that it has a global minimum at $(x, y) = (0, 0)$ with value $V(0, 0) = 0$. Hence the level curves of V are ovals that enclose the level "curve" $V^{-1}(0) = \{(0, 0)\}$ (see Figure 22).

For any trajectory $(x(t), y(t))$ of (13) a function of t is defined by $V(x(t), y(t))$.

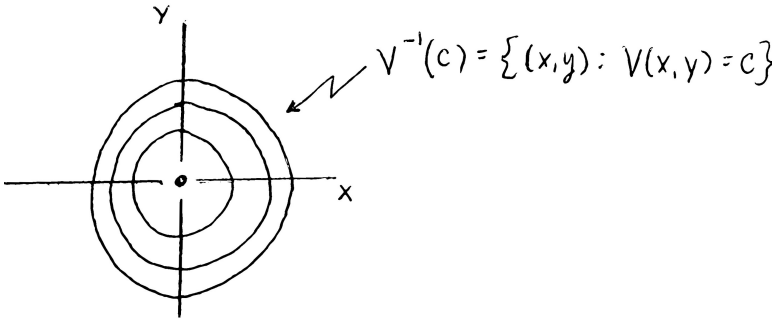

Figure 22: The Ovals That Enclose The Level Curve $V^{-1}(0)$

Then

$$\begin{aligned}\frac{d}{dt}[V(x(t),y(t))] &= G'(x(t))\dot{x}(t) + y(t)\dot{y}(t)\\ &= g(x)(y - F(x)) + y(-g(x))\\ &= -g(x(t))F(x(t)).\end{aligned}$$

This indicates that at any point (x, y) the instantaneous rate of change in V along the trajectory through (x, y) is

$$\dot{V}(x,y) \stackrel{\text{def}}{=} -g(x)F(x) \tag{15}$$

Since, as already noted, $g(x)$ has the sign of non-zero x, by the first hypothesis on $F(x)$

$$\dot{V}(x,y) > 0 \text{ on } \{(x,y) : \alpha < x < \beta \text{ and } x \neq 0\}$$

Thus, on a neighborhood of $(0, 0)$, $\dot{V}(x, y) \geq 0$. Hence, for some sufficiently small $V_0 > 0$, the flow of (13) is from the interior to the exterior of the oval $V^{-1}(V_0)$ (see Figure 23).

We want to show that if $y_1 > 0$ is sufficiently large, then the positive semi-orbit $O_+(0, y_1)$ intersects the negative y-axis and does so at a point $(0, y_2)$ that is closer to

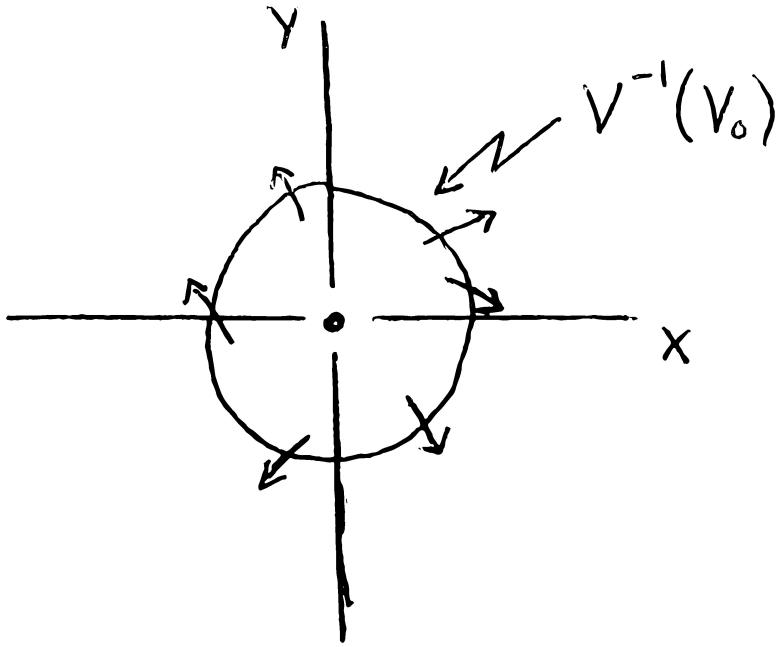

Figure 23: The Flow From The Interior to The Exterior of $V^{-1}(V_0)$

the origin that $(0, y_1)$ is. We will do this by showing that $V(0, y_2) = \frac{1}{2}(y_2)^2$ is smaller than $V(0, y_1) = \frac{1}{2}(y_1)^2$, which we do by studying the integral of $\dot{V}$ along $O_+(0, y_1)$ from $(0, y_1)$ to $(0, y_2)$.

It is clear that

$$\dot{x} = 0 \text{ along } y = F(x)$$

$$\dot{y} = 0 \text{ along } x = 0$$

and that these two curves divide the plane into four regions with directions of flow as indicated in Figure 24.

Since F takes negative values on the interval $(0, \beta)$ but $\lim_{x\to\infty} F(x) = +\infty$, by the Intermediate Value Theorem for any $y_1 > 0$ the horizontal line through the point $(0, y_1)$ must intersect the graph of $y = F(x)$ at a point whose abscissa is positive.

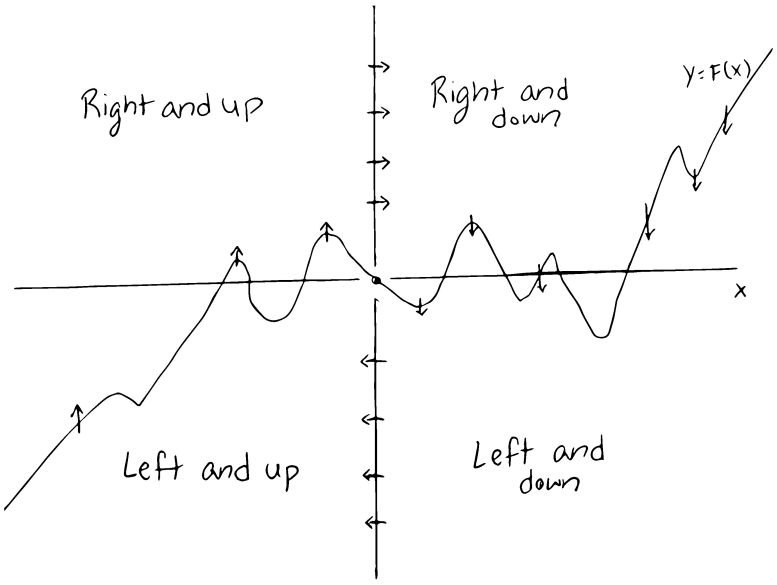

Figure 24: The Four Regions of The Plane With Directional Flow

Clearly it first does so at a point at which the function F is increasing. Thus the region S shown in Figure 25 is formed, with direction field on the boundary as indicated. But then, by Lemma 12, since the orbit through $(0, y_1)$ immediately enters S, the positive semi-orbit $O_+(0, y_1)$ through $(0, y_1)$ must leave S, and can do so only at a point on the graph of $y = F(x)$, hence it must intersect the graph of $y = F(x)$ at some point (a, b) with $a > 0$, as shown in Figure 29.

Claim 1:

Let (a, b) be any point on the curve $y = F(x)$, with $a > 0$. Then the forward orbit through (a, b), which we denote by $O_+(a, b)$, has non-empty intersection with the negative y-axis.

To prove the claim, let R denote the open region $\{(x, y) : 0 < x < a \text{ and } y < F(x)\}$

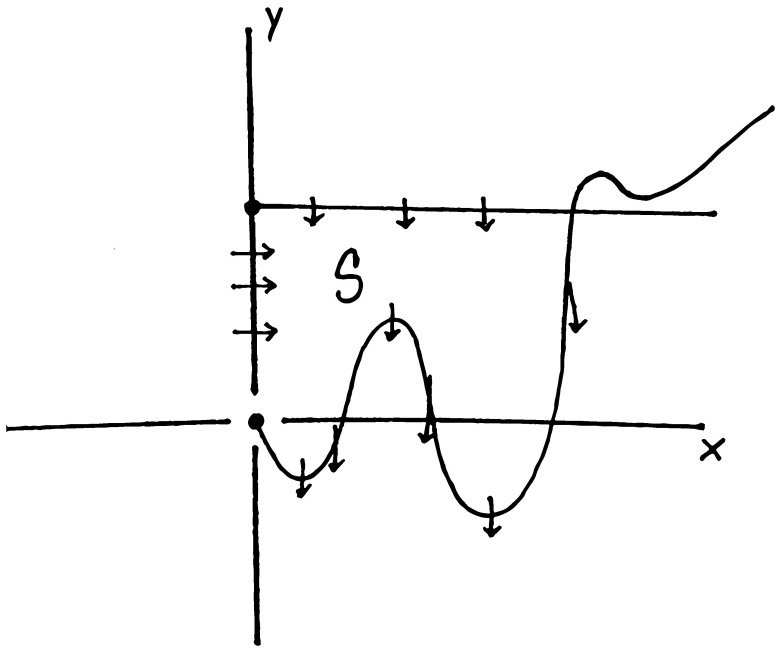

Figure 25: The Region S With Direction Field on The Boundary

as shown in Figure 26. The positive orbit $O_+(a,b)$ immediately enters R, throughout which $\dot{x} = y - F(x) < 0$ and $\dot{y} = -g(x) < 0$. Let ℓ denote the horizontal line with equation $y = min\{F(x) : x > 0\} - 1$, which divides R into two regions R_+ and R_-, as shown in Figure 27.

By Lemma 12, $O_+(a,b)$ must exit the region $\mathbb{R}_+$. There are two cases: either

$$(i)\ \ O_+(a,b) \cap (R \cap \ell) = \varnothing, \text{ or}$$

$$(ii)\ \ O_+(a,b) \cap (R \cap \ell) \neq \varnothing.$$

If case (i) holds, so that $O_+(a,b)$ does not exit R_+ across the segment $R \cap \ell$, then it must exit across the negative y-axis, so the proof of this case is complete.

Suppose (ii) holds, so that $O_+(a,b)$ intersects the segment $R \cap \ell$ at some point (a_1, b_1), hence immediately enters region R_-. Since ℓ has equation $y = min\{F(u) :$

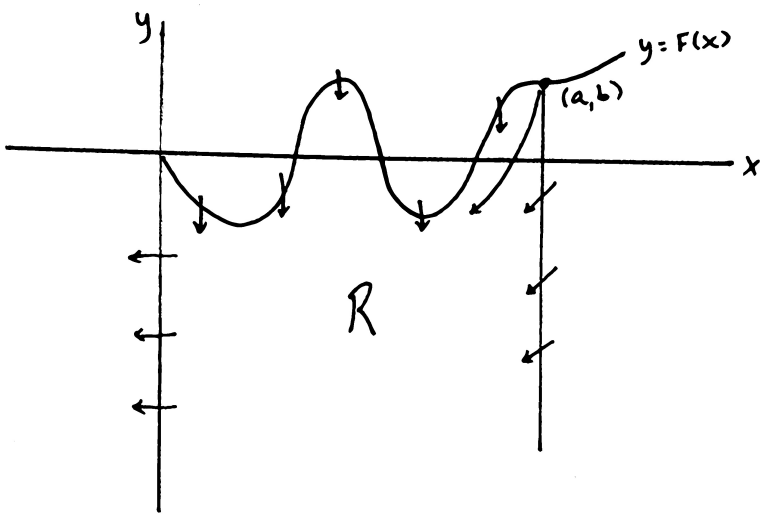

Figure 26: The Open Region $\{(x, y) : 0 < x < a \text{ and } y < F(x)\}$

$u > 0\} - 1$, at any point $(x, y) \in R_-$, $y < min\{F(u) : u > 0\} - 1 \leq F(x) - 1$, so $F(x) - y > 1$. But then the slope of the line tangent to the trajectory through the point (x, y) satisfies

$$\frac{dy}{dx} = \frac{\dot{y}}{\dot{x}} = \frac{-g(x)}{y - F(x)} = \frac{g(x)}{F(x) - y} < \frac{g(x)}{1} = g(x)$$

since $g(x)$ is positive in R. But then at any point $(a_2, b_2) \in O_+(a_1, b_1) \cap R_-$ (see Figure 28), integrating in the direction of increasing x,

$$b_1 - b_2 = \int_{a_2}^{a_1} \Big(\frac{dy}{dx}\Big) dx < \int_{a_2}^{a_1} g(x)dx = G(a_1) - G(a_2) < G(a_1)$$

since $G(a_2) > 0$, or $b_2 > b_1 - G(a_1)$. That is, as long as $O_+(a_1, b_1)$ remains in R_-, it is above the line ℓ' with equation $y = b_1 - G(a_1)$, hence cannot leave the portion of

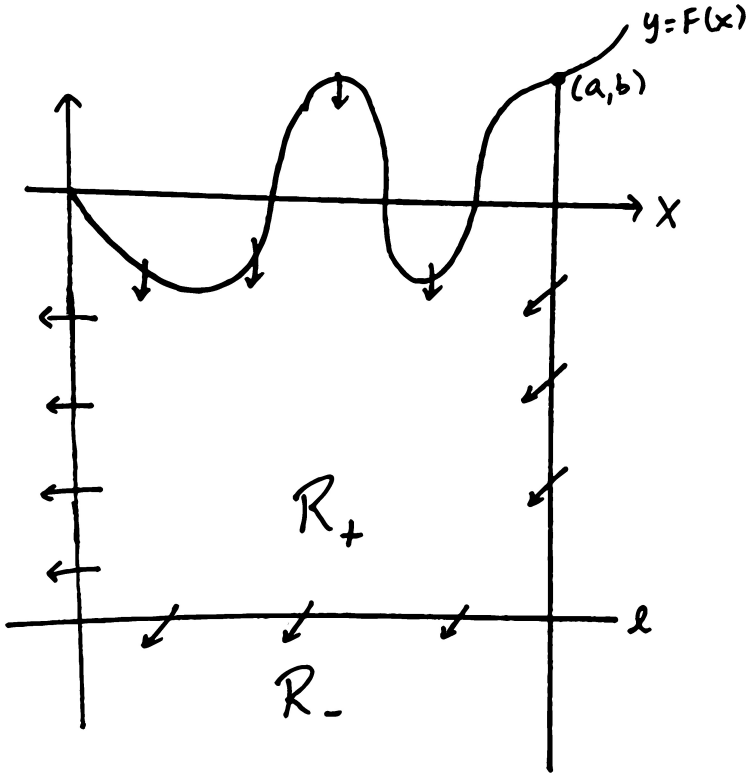

Figure 27: Line ℓ Divides R Into Regions R_+ and R_-

R_- between the lines ℓ and ℓ' except at a point on the negative y-axis. See Figure 28. But by Lemma 12, $O_+(a_1, b_1)$ must exit the region of R_- between ℓ and ℓ', finishing the proof of the claim for case (ii). This shows that the point $(0, y_2)$, the intersection of $O_+(0, y_1)$ with the negative y-axis, exists.

We note that exactly the same kind of reasoning used to prove Claim 1 establishes:
Claim 2: Let (a, b) be as in Claim 1. Then $O_-(a, b)$ has non-empty intersection with the positive y-axis.

We must now show that for $y_1 > 0$ sufficiently large, $V(0, y_1) - V(0, y_2) > 0$. As $y_1 > 0$ increases without bound, certainly $V(0, y_1) > 0$ increases without bound. Thus if $y_2 < 0$ does not tend to $-\infty$ but is bounded below, then $V(0, y_2) > 0$ is bounded above, and the desired inequality $V(0, y_1) - V(0, y_2) > 0$ must eventually

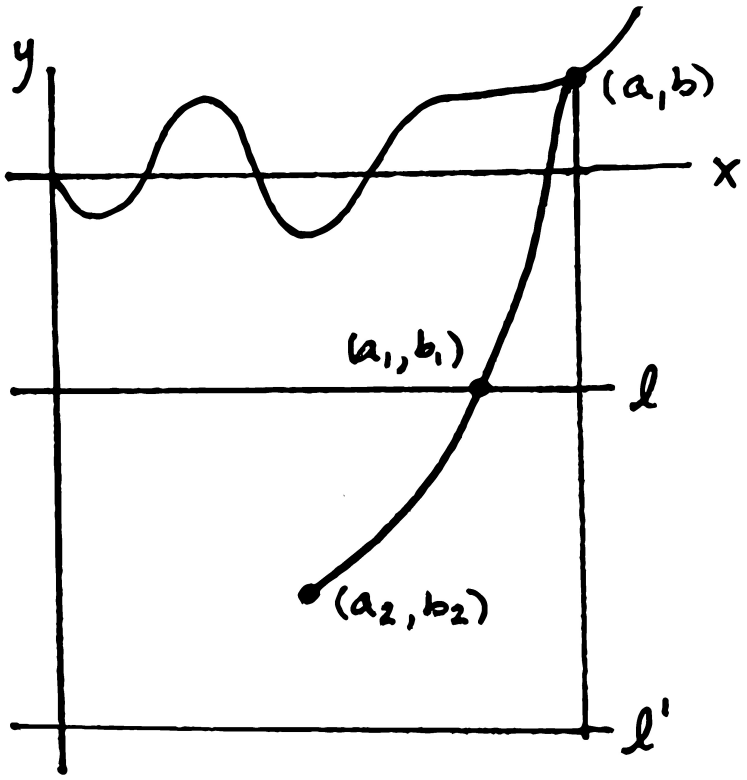

Figure 28: The Point (a_2, b_2) in the Region $O_+(a_1, b_1) \cap R_-$

hold. Thus we proceed under the assumption that $y_2 \to -\infty$ as $y_1 \to \infty$.

Since $\lim_{x\to\infty} F(x) = +\infty$ there exists a number $\gamma > 0$ such that $F(x) > 1$ for all $x > \gamma$. It follows from Claim 2 that for all sufficiently large $y_1 > 0$, $O_+(0, y_1)$ intersects the vertical line $x = \gamma$ before meeting the vertical isocline $y = F(x)$, and by Claim 1 that $O_+(0, y_1)$ intersects $x = \gamma$ a second time after it crosses $y = F(x)$ (see Figure 29).

The portions of $O_+(0, y_1)$ in the vertical strip $0 \le x \le \gamma$ are the graphs of functions (for $O_+(0, y_1)$ has no vertical tangents except where it crosses $y = F(x)$). So we may write

$$y = y_U(x) \text{ [U for "upper"]}$$

$$y = y_L(x) \text{ [L for "lower"].}$$

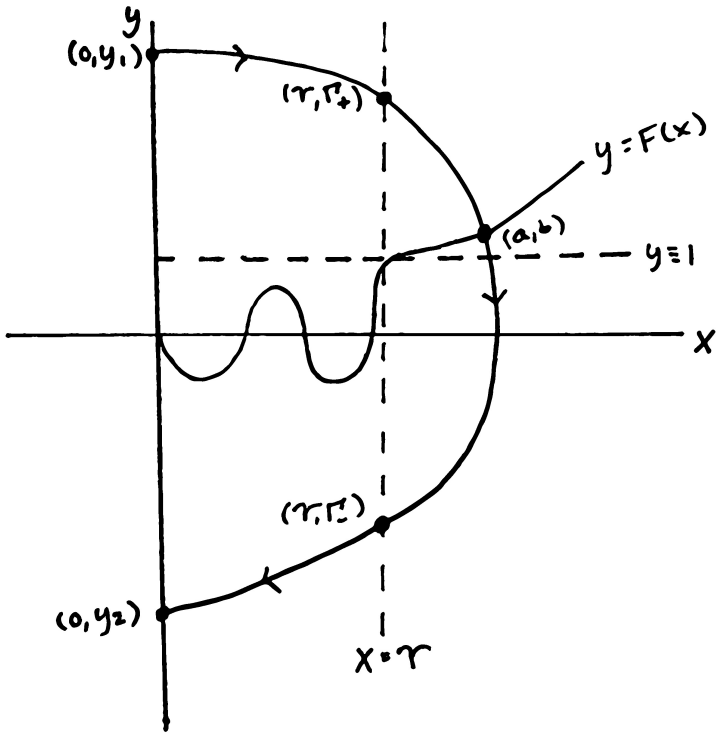

Figure 29: For y_1 Sufficiently Large

Let the coordinates of the points at which $O_+(0, y_1)$ intersects the line $x = \gamma$ be first (γ, Γ_+), then (γ, Γ_-).

Let the times that $O_+(0, y_1)$ is at its two intersections with $x = \gamma$ be

$$T_+ : (\gamma, \Gamma_+) = \Phi(T_+, (0, y_1))$$

$$T_- : (\gamma, \Gamma_-) = \Phi(T_-, (0, y_1)).$$

Let the time that $O_+(0, y_1)$ is at the point $(0, y_2)$ be T: $(0, y_2) = \Phi(T, (0, y_1))$. Now compute $V(0, y_2) - V(0, y_1)$ by integrating $\frac{d}{dt}[V(\Phi(t, (0, y_1)))]$ from $t = 0$ to $t = T$:

$$\begin{aligned} V(0, y_2) - V(0, y_1) &= V(\Phi(T, (0, y_1))) - V(\Phi(0, (0, y_1))) \\ &= \int_0^T \dot{V}(\Phi(t, (0, y_1)))dt \\ &= \int_0^T -g(x(t))F(x(t))dt \end{aligned}$$

by (15), where we have written $\Phi(t,(0,y_1)) = (x(t),y(t))$. We now split the integral into three parts, according to the division of the solution arc by the points (γ,Γ_+) and (γ,Γ_-). For the first and third arcs we write $dx = x'(t)dt = (y(t) - F(x(t))dt$ so that $dt = \frac{dx}{y-F(x)}$, thus obtaining

$$\begin{aligned} V(0,y_2) - V(0,y_1) = &\int_0^\gamma \frac{-g(x)F(x)}{y_U(x) - F(x)}dx - \int_0^\gamma \frac{-g(x)F(x)}{y_L(x) - F(x)}dx \\ &+ \int_{T_+}^{T_-} -g(x(t))F(x(t))dt \end{aligned} \tag{16}$$

where the minus sign in the second term arises from the direction of flow along the third arc opposing the direction of increasing x. Now consider the behavior of the sum as y_1 increases without bound. Independently of the value of y_1, the numerators in the first two summands are the same, unchanging continuous function on the closed and bounded interval $[0,\gamma]$, hence are bounded. The denominators both tend to zero with increasing y_1, the one in the second summand because we have been able to restrict to the assumption that $y_2 \to -\infty$ as $y_1 \to +\infty$. Thus the sum of the first two summands tends to zero as y_1 increases without bound. For the third summand in (16) we will manipulate differentials in $\dot{y} = \frac{dy}{dt} = -g(x)$ to write the third integral as

$$\begin{aligned} \int_{T_+}^{T_-} -g(x(t))F(x(t))dt = &\int_{\Gamma_+}^{\Gamma_-} F(x)dy \\ &= -\int_{\Gamma_-}^{\Gamma_+} F(x)dy, \end{aligned} \tag{17}$$

using the fact that x is a function of y on this arc of $O_+(0,y_1)$. But for x-values on this solution arc, $F(x) \geq 1$, hence by (17) we conclude that $\int_{T_+}^{T_-} -g(x(t))F(x(t))dt \leq -(\Gamma_+ - \Gamma_-)$. But from Figure 29 it is clear that $(\Gamma_+ - \Gamma_-) \to +\infty$ as $y_1 \to +\infty$, hence the third summand in (17) tends to $-\infty$, and we conclude from (17) that for

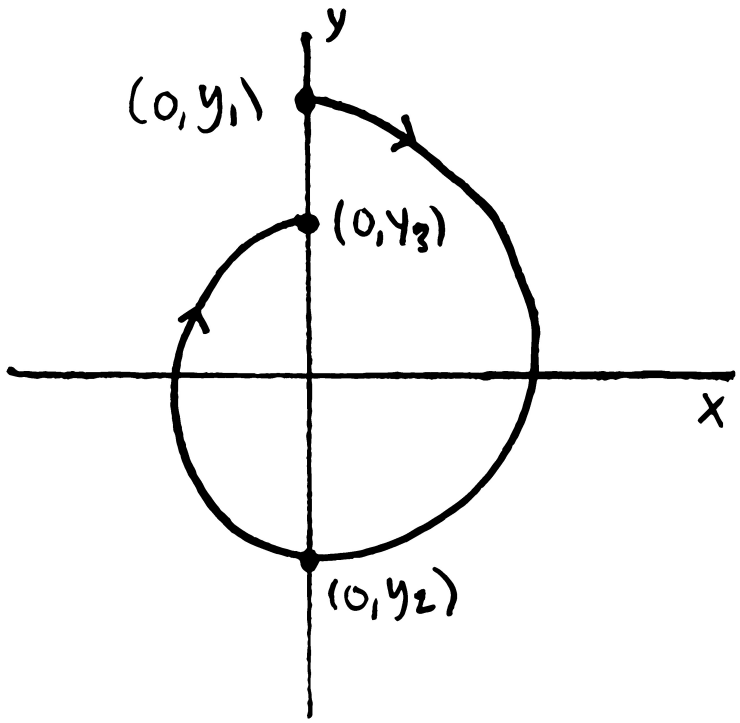

Figure 30: For $|y_2|$ Sufficiently Large

$y_1 > 0$ sufficiently large, $V(0, y_2) - V(0, y_1) < 0$.

The same line of reasoning shows that $O_+(0, y_2)$ meets the positive y-axis at a point $(0, y_3)$, and for $|y_2|$ sufficiently large, $|y_2| > y_3$, making Figure 30 correct. Thus the situation is as shown in Figure 31, where the small oval surrounding $(0, 0)$ is that of Figure 23, across which the flow is from the interior to the exterior. The closed region U bounded by this small oval and the closed curve form by the solution arc from $(0, y_1)$ to $(0, y_3)$ together with the subinterval $[y_3, y_1]$ in the y-axis is a compact, positively invariant set that contains no critical point. Select any point $(0, \bar{y})$ with $y_3 < \bar{y} < y_1$. $O_+(0, \bar{y})$ immediately enters and permanently remains in U, hence by the Poincaré-Bendixson Theorem (Theorem 7) the ω-limit set of $(0, \bar{y})$ is a closed orbit in U, since it does not contain a critical point, and the theorem is proved. $\square$

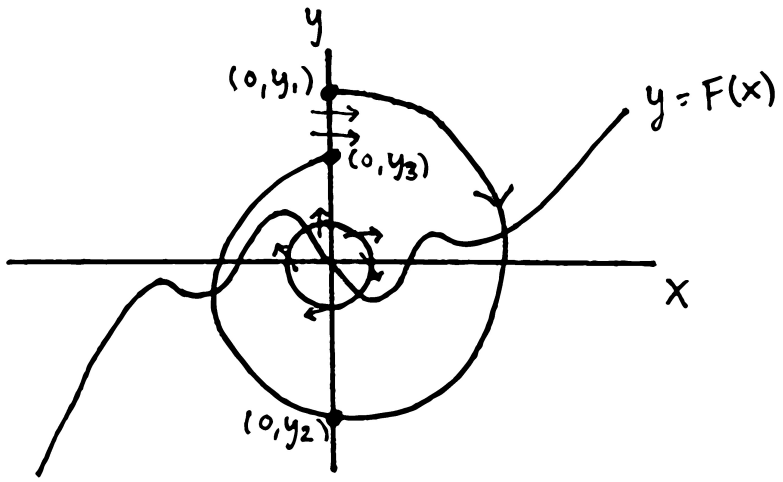

Figure 31: The Derived Region U

A number of variations of Liénard's Theorem have been proved over the years. Here we state just one, without proof, which has much more restrictive hypothesis than Theorem 12, but yields uniqueness of the cycle.

Theorem 13. Given $\ddot{x} + f(x)\dot{x} + g(x) = 0$, suppose f and g are C^r, $r \geq 1$, and that

1) $xg(x) > 0$ for $x \neq 0$

2) $g(x) = -g(-x)$, $f(x) = f(-x)$

and that for some $b > 0$, $F(x) = \int_0^x f(s)ds$ satisfies

a) $F(x) < 0$ if $0 < x < b$

b) $F(x) > 0$ if $x > b$, and

3) $F(x)$ is monotone increasing for $x > b$ and $F(x) \to \infty$ as $x \to \infty$

Then (12) has a unique nontrivial periodic solution.

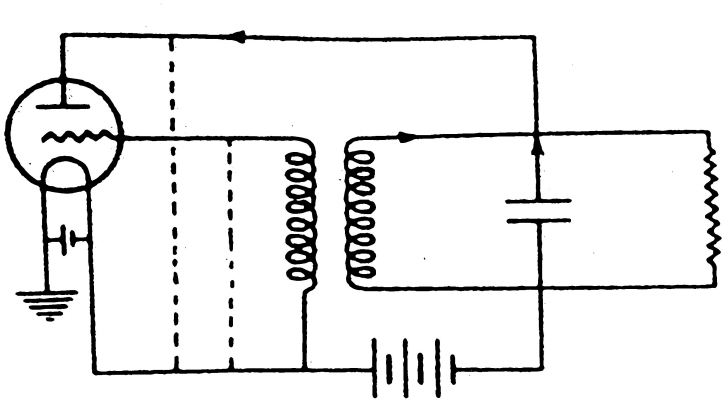

Figure 32: The van der Pol Triode Circuit

4.2 van der Pol Oscillator

While there are many different Liénard equations, one of the most important ones was formulated by Dutch physicist Balthasar van der Pol in 1927 to describe oscillations in a radio circuit. He experimented with these oscillations in a vacuum tube triode circuit as in Figure 32. This equation is of great historical importance because it is the first mathematical model of a real world system exhibiting a limit cycle. It is also a "self-sustained" oscillation because the energy that is put in is not oscillatory. The second order ordinary differential equation derived by van der Pol, now called the van der Pol equation, is as follows:

$$\ddot{x} + \mu(x^2 - 1)\dot{x} + x = 0. \tag{18}$$

For the system that van der Pol was modelling, $\mu > 0$. It is clear that x plays the role of a restoring force while $\mu(x^2 - 1)\dot{x}$ plays the role of a dampening force. We can see that if $|x| < 1$ then energy is being supplied to the system, (amplification by the triode tube), whereas, if $|x| > 1$ then energy is being dissipated (resistance).

It is easy to see that the van der Pol equation satisfies the hypothesis of Theorem 12, hence has at least one stable limit cycle in its phase portrait. We will prove that the cycle in the van der Pol System is unique. We could merely point out that (18) satisfies the hypothesis of Theorem 13, but will instead demonstrate the use of Theorem 11, which we have proved. To do so we transform (18) into a two-dimensional first order system by the standard introduction of a second dependent variable $y = \dot{x}$, thus obtaining

$$\begin{aligned} \dot{x} &= y \\ \dot{y} &= -x - \mu(x^2 - 1)y. \end{aligned} \tag{19}$$

If r is the radial polar coordinate, then

$$r\dot{r} = x\dot{x} + y\dot{y} = -\mu(x^2 - 1)y^2.$$

Thus, $\dot{r} > 0$ everywhere along the strip $-1 < x < 1$, except along the y-axis, and in particular the flow is everywhere outward across the unit circle $x^2 + y^2 = 1$, except possibly at the two points $(-1, 0)$ and $(1, 0)$, at which points the vector $X(x, y)$ corresponding to (19) is vertical. However, as Figure 33 shows, if $O_+(1, 0)$ does not immediately exit the unit disk, then an application of Lemma 12 to the negative semi-orbit of points on the boundary of the region S thus formed by $O_+(1, 0)$, the unit circle, and the line $y = -\bar{y}$ for small $\bar{y} > 0$ yields a contradiction. Similarly for $O_+(-1, 0)$. Now consider the annular region $A = \{(x, y) : x^2 + y^2 > 1\}$, in which any cycle of (19) must lie and on which the Dulac function $B(x, y) = (x^2 + y^2 - 1)^{-\frac{1}{2}}$

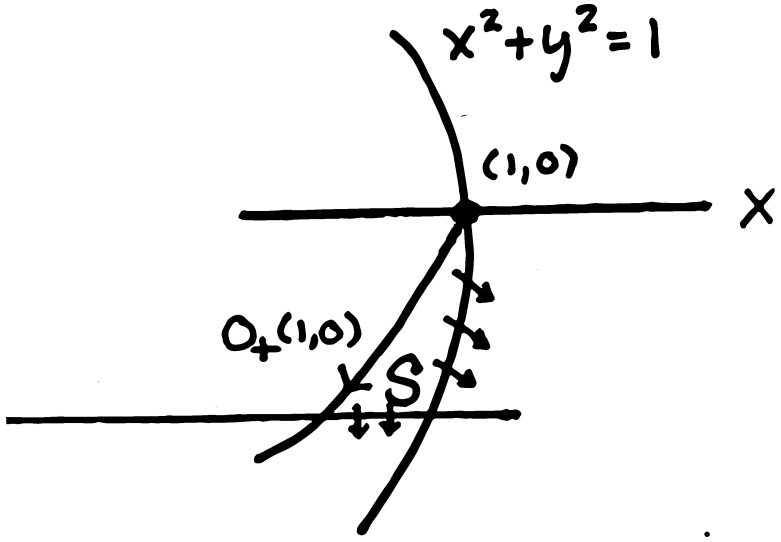

Figure 33: The Region S Formed by $O_+(1,0)$

(discovered by Leonid Cherkas in the 1990's) exists and is differentiable. We compute

$$\begin{aligned} div(BX) &= \frac{\partial}{\partial x}[y(x^2+y^2-1)^{-\frac{1}{2}}] + \frac{\partial}{\partial y}[(-x-\mu(x^2-1)y)(x^2+y^2-1)^{-\frac{1}{2}}] \\ &= -\frac{1}{2}y(x^2+y^2-1)^{-\frac{3}{2}}2x - \mu(x^2-1)(x^2+y^2-1)^{-\frac{1}{2}} \\ &\quad -\frac{1}{2}(-x-\mu(x^2-1)y)(x^2+y^2-1)^{-\frac{3}{2}}2y \\ &= (x^2+y^2-1)^{-\frac{3}{2}}[-xy-\mu(x^2-1)(x^2+y^2-1)-(-xy-\mu(x^2-1)y^2)] \\ &= (x^2+y^2-1)^{-\frac{3}{2}}[-\mu(x^2-1)(x^2-1)] \\ &= -\mu(x^2-1)^2(x^2+y^2-1)^{-\frac{3}{2}} \end{aligned}$$

which is not identically zero on any open subset of A and is of one sign on A. Thus by Theorem 11 the cycle of the van der Pol system that is guaranteed to exist by Liénard's Theorem (Theorem 12) is a unique limit cycle.

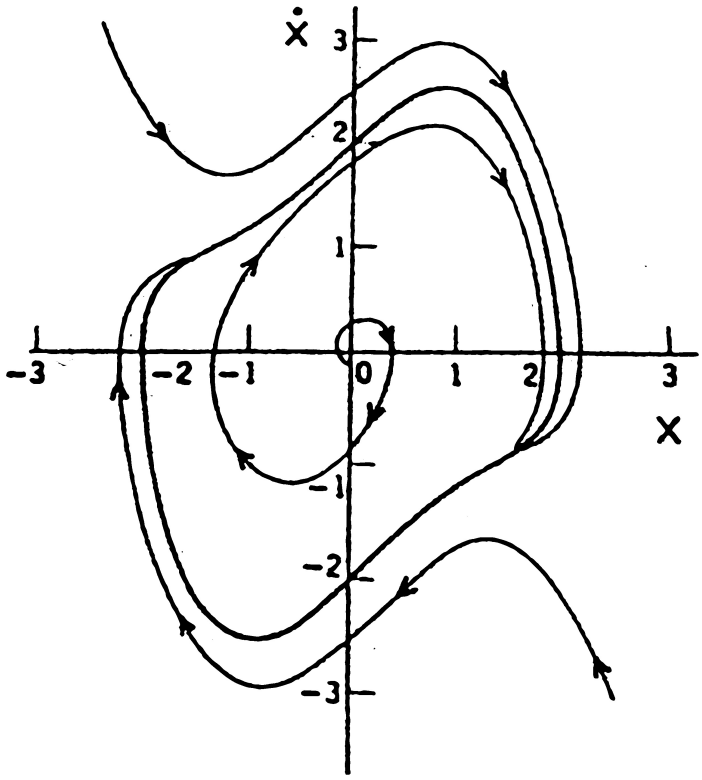

Figure 34: The Phase Portrait of the van der Pol Equation for $\mu = 1$

Now, to understand what the phase portrait for this equation looks like, let us take equation (18) and integrate numerically for $\mu = 1$. Figure 34 plots several solutions in the phase plane, which we see tend to the limit cycle. As μ increases, the limit cycle changes from a more circular cycle into a longer, more stretched out cycle. In Figure 34 we can see the beginning of this stretch, Figure 35 displays the nature of the graph of $x(t)$ for $\mu > 0$ large. In this graph, we can see why these oscillations are termed "relaxation oscillations". The graph "relaxes" after each jump in the graph before jumping once again.

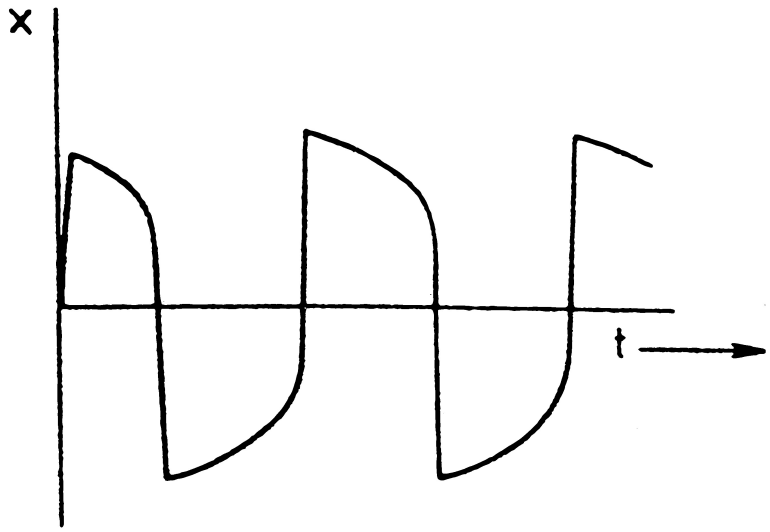

Figure 35: The van der Pol Relaxation Oscillation for $x = x(t)$

REFERENCES

[1] Ivar Bendixson. Sur les courbes définies par des equations différentielles. Acta Math. 24 (1901) 1-88.

[2] F. Brauer and J.A. Nohel. Qualitative Theory of Ordinary Differential Equations. New York: W. A. Benjamin Inc., 1969.

[3] C. Chicone and D.S. Shafer. Quadratic Morse-Smale vector fields which are not structurally stable. Proceedings Amer. Math. Soc. 85 (1982) 125-134.

[4] H. Dulac. Sur les cycles limites. Bull Soc. Math. France 51 (1923) 45-188.

[5] Alfred Liénard. Étude des oscillations entretenues, Revue Générale de l'Électricité 23 (1928) 901-912, 946-954.

[6] A.J. Lotka. Undamped oscillations derived from the law of mass action. J. Amer. Chem. Soc. 42 (1920) 1595-1599.

[7] A.J. Lotka. Elements of Physical Biology Baltimore: Williams and Wilkins, 1925.

[8] Lawrence Perko. Differential Equations and Dynamical Systems. Texts in Applied Mathematics 7. New York: Springer-Verlag, 1991, 1996, 2001.

[9] Henri Poincaré. Sur les courbes définie par les équations différentielles. C. R. Acad. Sci. 90 (1880) 673-675.

[10] Henri Poincaré. Mémoire sur les courbes définie par une équation différentielle. I, II, III, and IV, J.Math. Pures Appl. 7 (1881) 375-422; 8 (1882) 251-286; 1 (1885) 167-244; 2 (1886) 151-217.

[11] S.H. Strogatz. Nonlinear Dynamics and Chaos. Boston: Addison-Wesley Publishing Company, 1994.

[12] Balthasar van der Pol. On relaxation-oscillations, Philos. Mag. 2 (1926) 978-992.

[13] Balthasar van der Pol. Forced oscillations in a circuit with nonlinear resistance (receptance with reactive triode), London, Edinburgh, and Dublin Phil. Mag. 3 (1927) 65-80.

[14] Ferdinand Verhulst. Nonlinear Differential Equations and Dynamical Systems. New York: Springer-Verlag, 1990.

[15] V. Volterra. Variazionie fluttuazioni del numero d'individui in specie animali conviventi. Mem. Acad. Lincei 2 (1926) 31-113. (Variations and Fluctuations of a number of individuals in animal species living together. Translation in: R.N. Chapman. Animal Ecology. New York: McGraw-Hill, 1931, pp 409-448.)

[16] Y.-Q. Ye. Theory of Limit Cycles.Translations of Mathematical Monographs Vol 66. Providence, RI: American Mathematical Society, 1986.